Greenhouse conditions in Lower Eocene coastal wetlands? – Lessons from Schöningen, Northern Germany

Olaf K. Lenz[1], Walter Riegel[2], Volker Wilde[2],

[1]General Directorate, Senckenberg Society for Nature Research, Frankfurt am Main, Germany.

[2]Department Palaeontology and Historical Geology, Senckenberg Research Institute and Natural History Museum, Frankfurt am Main, Germany.

*Corresponding author

E-mail: olaf.lenz@senckenberg.de (OL)

Author contributions

Conceptualization: Olaf K. Lenz, Walter Riegel, Volker Wilde

Data Curation: Olaf K. Lenz

Formal Analysis: Olaf K. Lenz

Funding Acquisition: Olaf K. Lenz

Investigation: Olaf K. Lenz, Walter Riegel, Volker Wilde

Methodology: Olaf K. Lenz, Walter Riegel, Volker Wilde

Project Administration: Olaf K. Lenz, Volker Wilde

Resources: Olaf K. Lenz, Walter Riegel, Volker Wilde

Validation: Olaf K. Lenz

Visualization: Olaf K. Lenz

Writing – Original Draft Preparation: Olaf K. Lenz

Writing – Review & Editing: Walter Riegel, Volker Wilde

Abstract

The Paleogene succession of the Helmstedt Lignite Mining District in Northern Germany includes coastal peat mire records from the latest Paleocene to the middle Eocene at the southern edge of the Proto-North Sea. Therefore, it covers the different long- and short-term climate perturbations of the Paleogene greenhouse. 56 samples from three individual sections of a Lower Eocene seam in the record capture the typical succession of the vegetation in a coastal wetland during a period that was not affected by climate perturbation. This allows to distinguish facies-dependent vegetational changes from those that were climate induced. Cluster analyses and NMDS of well-preserved palynomorph assemblages reveal four successional stages in the vegetation during peat accumulation: (1) a near-coastal vegetation, (2) a lowland mire, (3) a transitional mire, and (4) a terminal mire. Biodiversity measures show that plant diversity decreased significantly in the successive stages. The highly diverse vegetation at the coast and in the adjacent lowland mire was replaced by low diversity communities adapted to wet acidic environments and nutrient deficiency. The palynomorph assemblages are dominated by elements such as *Alnus* or *Sphagnum*. Typical tropical elements which are characteristic for the Middle Eocene part of the succession are missing. This indicates that a more temperate climate prevailed in northwestern Germany during the early Lower Eocene.

Introduction

The long-term warming trend of the early Paleogene greenhouse climate climaxed in the Early Eocene Climatic Optimum (EECO) between *c.* 52 and 50 Ma before present (BP) [1]. It was interrupted by short-term warming events, the most prominent of which was the Paleocene-Eocene Thermal Maximum (PETM or ETM-1, e.g., [2-4]), a sudden temperature peak at the transition from the Paleocene to the Eocene, which is estimated to have lasted about 170.000 years [5]. Other short-term events followed, such as the ETM-2 (*c*. 53.6 Ma BP [6,7]) and the ETM-3 (X- or K-event; *c*. 52.5 Ma BP [8,9]), but did not reach the intensity of the PETM.

The sedimentary succession of the former Helmstedt Lignite Mining District, which includes the mines at Schöningen, covers the entire Paleogene greenhouse phase and its gentle demise from the latest Paleocene to the Middle Eocene in the so-called Helmstedt Embayment at the southern edge of the Proto-North Sea. This offers the unique opportunity to trace the effects of all the long- and short-term climate perturbations on Paleogene terrestrial ecosystems across more than 10 million years. The study is part of a current project on changes in composition of the vegetation and plant diversity in the coastal environment of the Helmstedt Embayment across the EECO and its short-term perturbations such as the PETM and ETM-2 by using pollen and spores as proxies.

In a number of previous studies, we have shown how the repeated and often rapid changes from marginal marine to estuarine, fluvial and terrestrial in the Late Paleocene to Middle Eocene succession at Helmstedt and Schöningen are accompanied by great changes in vegetation [10-12]. However, a climatic influence and the corresponding response of the ecosystems cannot simply be revealed from the microflora as documented in the record of the Helmstedt Lignite Mining District. Multiple alternations of lignites with marine and fluvial interbeds in the section indicate significant

facies changes which should have been coupled with changes in vegetation. When studying climate changes and perturbations in the palynomorph record it is therefore necessary to distinguish between facies-dependent changes and changes which are merely climate-induced.

Isotope analyses from the lower part of the Schöningen Formation revealed an isotope excursion from the top of Seam 1 to the middle of Seam 2 including Interbed 2 [13]. As yet, it remains unclear, however, which of the Early Eocene warming events it represents and which specific floral elements are associated with the event. Carbon isotope values do not indicate a CIE excursion for Seam 1 except for the uppermost sample [13]. Therefore, Seam 1 has been deposited during a period without any perturbations of the climate and changes in vegetation were controlled by factors other than climate such as edaphic effects. Since palynological data from adjacent seams at Schöningen show similar assemblage composition and vertical trends, our data from Seam 1 can be taken as representative for a coastal plain vegetation at the southern edge of the Early Eocene Proto-North Sea. This opens the opportunity to determine more precisely the composition of the regional flora outside of warming events and its variability prior to identifying strictly climatic signals. We selected Seam 1, for which three individual sections were available from the Schöningen outcrops and studied them palynologically including multivariate statistical analyses and biodiversity measures.

Geological setting

The Helmstedt Lignite Mining District is situated within the Paleogene Helmstedt Embayment, which represented the mouth of an estuary opening towards the Proto-North Sea (Fig 1) between major uplifts corresponding to the actual Harz Mountains to the South and the Flechtingen Rise to

the North [14]. The estuary at some times extended far inland towards the area of Halle and Leipzig (Leipzig Embayment [15, 16]). Due to the interaction between changes in sea level, salt withdrawal in the subsurface and climate-related changes in runoff from the hinterland the area of Helmstedt and Schöningen was subject to frequent changes between marine and terrestrial conditions, repeatedly leading to peat formation [17].

Fig 1. Paleogeographic map of Northwestern Europe during the Lower Eocene. The map shows the Helmstedt Embayment at the southern edge of the Proto-North Sea (H) in relation to important middle Eocene fossil localities in Germany, such as the Geiseltal (G), Messel (M), and Eckfeld (E).

Today, the Paleogene deposits of the Helmstedt Lignite Mining District are limited to two marginal synclines accompanying the more than 70 km long salt wall of Helmstedt-Staßfurt [14, 18]. Both of the synclines are strongly asymmetric with steeply inclined strata away from a narrow core of Zechstein rocks while they are gently dipping on the opposite flanks. The influence of salt-withdrawal on sediment accumulation is indicated by the fact that the maximum thickness of the two lignite bearing sequences and of the individual coal seams moved towards the salt-wall with time [14, 18].

Stratigraphy

An approximately 400 m thick Paleogene succession in both synclines unconformably follows on Mesozoic sediments of Triassic and Lower Jurassic age (Fig 2). The position of the lignites and two major marine transgressions in the sequence suggested a subdivision of the Paleogene strata from bottom to top in Underlying Sediments (now Waseberg Formation), Lower Seam Group (now

115 Schöningen Formation), Emmerstedt Greensand (now Emmerstedt Formation), Upper Seam Group
116 (now Helmstedt Formation) and Overlying Marine Strata (now Annenberg-, Gehlberg-, und
117 Silberberg Formations) (Fig 2) [11,19,20].
118
119 **Fig 2**. **Stratigraphic scheme of the Paleogene succession in the Western and Eastern Syncline**
120 **at Helmstedt and Schöningen.** The age model for the succession is based on K/Ar-ages [19,21],
121 nannoplankton zones [19], dinoflagellate zones [22] and palynological zones [23,24]. Data for
122 global changes in Paleogene sea-level [25] and higher order orbital cyclicity (long
123 eccentricity >589 Ma) [26] are used for a putative correlation to seams in the Schöningen Südfeld
124 section. The asterisk points to the stratigraphic position of the studied sections
125
126 The conventional age model (Fig 2) for the coal-bearing part of the Paleogene succession
127 of the Helmstedt Lignite Mining District is mainly based on scattered radiometric ages from
128 glauconites [19,21] as well as biostratigraphic data from nannoplankton [19], dinocysts [21,22] and
129 palynomorphs [23,24]. The data for the Schöningen-, Emmerstedt- and Helmstedt Formations were
130 mostly derived from wells near Helmstedt in the Eastern Syncline and have simply been transferred
131 to both synclines in the rest of the area. They suggest a Lower Eocene (Ypresian) age for the
132 Schöningen Formation and a Middle Eocene (Lutetian) age for the Helmstedt Formation.
133 More recent results on quantitative data for the dinoflagellate cyst genus *Apectodinium* and
134 carbon isotopes from the section at Schöningen in the western syncline indicate that the lowermost
135 part of the Schöningen Formation may still be of Paleocene age [11,13]. Furthermore, this age
136 model appears consistent when the succession of seams at Schöningen is compared to global
137 changes in Paleogene sea-level and higher order cyclicity [11].

The Schöningen Formation as exposed in the opencast mine Schöningen-Südfeld (Fig 3) of the Western Syncline has a thickness of about 155 m, including 9 almost continuous seams (Main Seam and Seam 1 to Seam 9) and some other seams of limited extent, including Seam "L" and the "*Sphagnum* Seam" [11,27]. The Emmerstedt Formation cannot be identified at Schöningen since the characteristic greensand is missing.

Fig 3. The Helmstedt Lignite Mining District. (A) The former opencast mines at Helmstedt and Schöningen. The blue frame marks the detail presented in (B). The red line indicates the salt wall separating the Western and Eastern Synclines. (B) The former opencast mines Schöningen Nordfeld and Schöningen Südfeld east of Schöningen. The positions of the three studied sections of Seam 1 are indicated.

Due to a lack of radiometric dates and relevant biostratigraphic information, the exact position of both, the Paleocene-Eocene boundary and the Ypresian-Lutetian boundary still remain unknown at Schöningen. The frequency of *Apectodinium* spp. just above Seam 1 [11,13] has been discussed as indicating the Paleocene-Eocene Thermal Maximum (PETM) (see [28-34]). However, the marker species of the PETM in open marine environments *A. augustum* [28], now *Axiodinium augustum* [35], is not found among the countless *Apectodinium* cysts above Seam 1 [13]. Furthermore, since *Apectodinium* acmes occur in marginal marine areas in the North Sea basin also at other times during the Early and Middle Eocene [36] the distinct carbon isotope excursion (CIE) co-occurring with the *Apectodinium* acme in Interbed 2 cannot unequivocally be related to the PETM and may point to another later warming event [13]. Thus, Seam 1, which is in the focus of our study, cannot be unambiguously dated at the moment.

Methods

Sampling and sample processing

Three sections of Seam 1 have been studied (Figs 3 and 4) in now abandoned opencast mines in the western syncline at Schöningen. Section N (14 samples) was located in mine Schöningen-Nordfeld (52°09'23.8"N 10°58'44.0"E), while the sections S1 (12 samples) and S2 (30 samples) were taken in mine Schöningen-Südfeld (S1: 52°08'07.1"N 10°59'29.7"E; S2: 52°08'27.9"N 10°59'24.5"E). The palynological data of sections S1 und S2 are based on new quantitative counts while the analysis of section N is based on unpublished data of Hammer-Schiemann (1998, unpublished dissertation, University of Göttingen).

Fig 4. Lithological logs of the three studied sections of Seam 1. Section N is located in mine Schöningen Nordfeld, sections S1 and S2 are from mine Schöningen Südfeld. Grain size distribution is based on field observation. Numbers indicate palynological samples.

Most of the lithological units of the lignite succession in the three sections are represented in the present study by a single sample at least. In order to include the interbed/seam transitions, seven samples from the underlying Interbed 1 and the succeeding Interbed 2 have been studied in addition (Fig 4).

Palynological preparation followed the standard procedures as described by [37] including the successive treatment with hydrochloric acid (HCl), hydrofluoric acid (HF), hydrogen peroxide (H_2O_2) and potassium hydroxide (KOH). Flocculating organic matter was removed by briefly oxidizing the residue with nitric acid (HNO_3) or hydrogen peroxide (H_2O_2) after sieving with a

mesh size of 10 µm. Remaining sample material and slides are stored at the Senckenberg Forschungsinstitut und Naturmuseum, Sektion Paläobotanik, Frankfurt am Main, Germany.

Quantitative palynological analysis

Numerical analyses of palynological data are based on quantitative palynomorph counts. At least 300 individual palynomorphs per sample were identified and counted at 400 times magnification to obtain a representative dataset for statistical analysis. A complete list of all palynomorphs encountered during the present study with full names including authors is presented in the taxonomic list (S1 Appendix). Furthermore, raw data values for section N (S1 Table), section S1 (S2 Table) and section S2 (S3 Table) are presented in the appendix. Identification of palynomorphs is based on the systematic-taxonomic studies of [10,38-41].

Despite the good preservation of palynomorphs 5-10% of the total assemblages could not be identified and have been counted as "Varia". To minimize potential errors in identification and counting of individual species some morphologically similar taxa have been lumped in the pollen diagrams and for statistical analysis, such as, e.g., different species of the genera *Triporopollenites* or *Triatriopollenites*. In total, 45 groups of palynomorphs have been distinguished (see S1 Appendix). In order to get robust data for diversity analyses the slides from section S1 were additionally scanned for rare taxa that were not recorded during routine counting.

The pollen diagrams show the abundance of the most important palynomorphs in percentages. They are arranged according to their score along the first axis (sections N, S2) or the second axis (section S1) of an NMDS gradient analysis. Pollen and spores were calculated to 100%, whereas algae, such as *Botryococcus*, dinoflagellates and other organic residues, such as fungal remains, cuticles or charcoal were added as additional percentages (in % of the total sum of pollen and spores).

Statistical analysis

Statistical analyses followed a routine which has already been applied by the authors in previous studies [42,43]. We used Wisconsin double standardized raw data values [44-47]. Wisconsin standardization scales the abundance of each taxon or group of taxa to their maximum values and represents the abundance of each of these palynological variables by its proportion in the sample [48]. This equalizes the effects of rare and abundant taxa and removes the influence of sample size on the analysis [44,45].

For the robust zonation of the pollen diagrams of the three sections and to identify samples with similar palynomorph contents, Q-mode cluster analysis was established using the unweighted pair-group average (UPGMA) method and the Bray-Curtis distance (software PAST 3.26 [49]). Furthermore, to illustrate compositional differences and ecological trends in Seam 1, and to visualize the level of similarity between samples, non-metric multidimensional scaling (NMDS) with the standardized raw data values and the Bray-Curtis dissimilarity [44,50] has been performed for each of the three studied sections as well as for the complete data set using the software PAST 3.26 [49]. NMDS is the most robust unconstrained ordination method in ecology [51] and has been successfully applied to palynological data in previous studies (e.g., [42,48,52-54]. It avoids the assumption of a linear or unimodal response model between the palynomorph taxa and the underlying environmental gradients as well as the requirement of normal distributed data.

Diversity analysis

In addition to the quantitative analysis of the 45 groups of palynomorphs that are presented in the pollen diagrams, in section S1 the palynomorph assemblage has been studied with the highest possible taxonomic resolution allowing a detailed analysis of the diversity of the microflora (S4 Table). For diversity analysis, morphologically distinct pollen “species” were recorded

representing the morpho-diversity of the palynomorph assemblage. However, these morpho-types do not necessarily reflect different parent plants and may also include morphological variation within the same plant family or genus. Furthermore, morphological diversity within a natural species may include different morpho-types [55]. Nevertheless, since this affects all samples to the same extent, the diversity measures still lead to a robust picture of the diversity of the parent vegetation.

To estimate the changes in taxonomic diversity between single samples and different pollen zones (PZs) within seam 1, several calculations for species richness and evenness were applied, using tools for biodiversity analysis as provided by [56,57]. Richness is simply the number of taxa within an ecosystem, which is here calculated as the total number of palynological taxa within a sample or a PZ [58]. It can be measured at different scales, for which mainly the three terms alpha, beta, and gamma diversity have been used [59]. The definitions of these terms were originally based on the comparison of diversity in different areas or regions. Here, we use these terms to describe the temporal comparison of diversity changes within Seam 1. Furthermore, we use the term point diversity (within-sample diversity resp. standing richness of [60]) for the richness within a single sample which reflects the total number of taxa as found in the counted number of individual grains [61]. Alpha diversity is regularly related to the diversity within a community or habitat [61] and is here used as a measure for diversity within a PZ, since this represents a specific community during the evolution of the vegetation in Seam 1. Gamma diversity normally includes the species richness in a larger area within a landscape [61] but is here used as a measure for the richness in the complete seam summarizing the vegetation of its peat-forming communities at Schöningen. Beta diversity is linking alpha and gamma diversities and is here used as a measure of the difference in species composition between two samples, within a specific PZ or within the whole seam [59,61-63]. Here we adapt Whittaker's [59,64] original suggestion for calculating beta diversity, which is

most frequently employed in ecological studies [65]. For comparison between two samples, beta diversity is calculated by the total number of species within the two samples divided by the average species number within the two samples. Beta diversity calculations within a PZ and within Seam 1 are calculated as the total species number within the specific PZ or the whole seam divided by the average species number in samples from the PZ/Seam 1. We applied software PAST 3.26 [49] for calculation of point and beta diversity as well as EstimatesS v. 9.1.0 [57] for the analysis of alpha and gamma diversity.

Species richness cannot directly be estimated by observation and not accurately measured, because the observed number of species in a sample is always a downward-biased estimator for the complete species richness in an assemblage [66]. Therefore, the calculation of the number of palynological species within a single sample or a PZ in the succession of Seam 1 is always an underestimate of the possible number of species. Nevertheless, the calculated richness values can be used as reliable information at least on relative changes of point and alpha diversity.

Evenness is the distribution of pollen taxa within a pollen assemblage [61]. A low evenness indicates an assemblage with one or more dominant taxa, characterized by high numbers of pollen grains of the same types, whereas high evenness points to an assemblage without dominant taxa, indicated by equally distributed taxa [67]. Evenness (E) has been calculated using the formula provided by [58] (E= H/ln(R)) producing evenness values between 0 (low evenness) and 1 (high evenness). For Shannon-Wiener index (H) and richness (R) we used the estimations provided by [56] based on calculations for point diversity within 300 counts, for alpha diversity within 5 samples and for gamma diversity within 20 samples (Tables 1 and 2).

Results

Palynozones

Based on unconstrained Q-mode cluster analysis (Figs 5B, 6B, 7B) five distinct assemblages have been recognized in our study, which can be distinguished by NMDS (Figs 5C, 6C, 7C). They are arranged as palynozones (PZ) in a vertical succession, which shows that the general development of the vegetation was identical in the three sections of Seam 1. Variations within PZs between sections indicate local differences in vegetation patterns.

Fig 5. Pollen diagram, cluster analysis and NMDS of section N. (A) Pollen diagram of 14 samples from the top of Interbed 1 to the base of Interbed 2 of section N showing the most important palynomorph taxa. The zonation in different PZs is based on cluster analysis (B) Result of an unconstrained cluster analysis of Wisconsin double standardized raw-data values using the unweighted pair-group average (UPGMA) method together with an Euclidean distance (C) Non-metric multidimensional scaling (NMDS) plot of palynological data using the Bray-Curtis dissimilarity and Wisconsin double standardized raw-data values. The scatter plot shows the arrangement of samples and palynomorph taxa.

Fig 6. Pollen diagram, cluster analysis and NMDS of section S1. (A) Pollen diagram of 12 samples from the base of seam 1 to the base of Interbed 2 of section S1 showing the most important palynomorph taxa. The zonation in different PZs is based on cluster analysis (B) Result of an unconstrained cluster analysis of Wisconsin double standardized raw-data values using the unweighted pair-group average (UPGMA) method together with an Euclidean distance (C) Non-metric multidimensional scaling (NMDS) plot of palynological data using the Bray-Curtis dissimilarity and Wisconsin double standardized raw-data values. The scatter plot shows the arrangement of samples and palynomorph taxa.

Fig 7. Pollen diagram, cluster analysis and NMDS of section S2. (A) Pollen diagram of 30 samples from the top of Interbed 1 to the base of Interbed 2 of section S2 showing the most important palynomorph taxa. The zonation in different PZs is based on cluster analysis (B) Result of an unconstrained cluster analysis of Wisconsin double standardized raw-data values using the unweighted pair-group average (UPGMA) method together with an Euclidean distance (C) Non-metric multidimensional scaling (NMDS) plot of palynological data using the Bray-Curtis dissimilarity and Wisconsin double standardized raw-data values. The scatter plot shows the arrangement of samples and palynomorph taxa.

PZ 1 and PZ 5 include samples from the adjacent Interbeds 1 and 2, and reflect the state of vegetation during marine-terrestrial transition. PZs 2, 3, and 4, on the other hand, represent different stages of the peat forming vegetation during seam formation.

Palynozone 1 (top Interbed 1)

The two samples from Interbed 1 (sample N-1, Fig 5A and sample S2-1, Fig 7A) show marine influence with the occurrence of dinocysts (*Apectodinium* spp.). The NMDS of S2 samples (Fig 7C) shows that sample S2-1 is clearly different from the seam, because it is plotted in the ordination space on the negative side of NMDS axis 2 together with samples of Interbed 2 (PZ 5) but separate from all of the lignite samples (PZ 2 - 4). Sample N-1 (section N, Fig 5C) is plotted in the upper right corner of the ordination space very close to samples from the base of Seam 1 (PZ 2a) indicating a more gradual change of the vegetation from marginal marine habitats to the peat-forming environment at this site.

323 The only true mangrove element *Rhizophora* (*Zonocostites ramonae,* Fig 8I), in the
324 Schöningen Formation, occurs in low numbers in PZ 1 of section S2 and in PZ 5 of sections S1
325 and S2. *Inaperturopollenites* spp. (Cupressaceae s.l., Figs 8A, B) dominate the pollen assemblages
326 with values of up to 37%. Other common taxa of sample N-1 are *Tricolporopollenites cingulum*
327 (Fagaceae, 9.4%, Figs 8C, D, E), *Plicatopollis* spp. (Juglandaceae, 7.7%, Fig 8K),
328 *Tricolpopollenites liblarensis* (Fagaceae, Fig 8F) and *T. retiformis* (Salicaceae, Fig, 8H), each with
329 5.1% as well as *Plicapollis pseudoexcelsus* (Juglandaceae?, 4.3%, Fig 8J).
330
331 **Fig 8. Important palynomorphs of PZs 1, 2 and 5**. (A) *Inaperturopollenites concedipites,*
332 Cupressaceae s.l. (sample S1-12), (B) *Cupressacites bockwitzensis,* Cupressaceae s.l. (sample S1-
333 12); (C) *Tricolporopollenites cingulum fusus,* Fagaceae (morphotype 1 with a rough exine, larger
334 than morphotype 2; sample S1-12), (D) *Tricolporopollenites cingulum fusus,* Fagaceae
335 (morphotype2 with a smooth exine, smaller than morphotype 1; sample S1-12), (E)
336 *Tricolporopollenites cingulum pusillus,* Fagaceae (morphotype 2, sample S1-9), (F)
337 *Tricolpopollenites liblarensis liblarensis,* Fagaceae (sample S1-12), (G) *Tricolpopollenites*
338 *quisqualis,* Fagaceae (sample S1-12); (H) *Tricolpopollenites retiformis,* Salicaceae (sample S1-4);
339 (I) *Zonocostites ramonae,* Rhizophoraceae (sample S1-8); (J) *Plicapollis pseudoexcelsus,*
340 Juglandales (sample S1-9); (K) *Plicatopollis hungaricus,* Juglandaceae (sample S1-3); (L)
341 *Alnipollenites verus,* Betulaceae (sample S1-3); (M) *Dicolpopollis kockeli,* Arecaceae (sample S1-
342 3); (N), (O) *Nyssapollenites kruschii accessories,* Nyssaceae (samples S1-12, S1-3); (P)
343 *Ilexpollenites iliacus,* Aquifoliaceae (sampleS1-4); scale bars: 10µm
344

In sample S2-1 *Plicatopollis* spp. (6.7%) and *P. pseudoexcelsus* (8.0%) are also very common, while the fagaceous taxa *T. liblarensis* and *T. cingulum* as well as *T. retiformis* are less frequent compared to sample N-1.

Palynozone 2 (Seam 1)

PZ 2 (Figs 5A, 6A, 7A) includes the lower part of Seam 1 and can be subdivided into two subzones in sections N and S2. The difference to other samples of the seam is best expressed in section S2 in the NMDS where samples of PZ 2 are clearly separate on the right side of the ordination space (Fig 7C). In the other two sections, samples from adjacent interbeds are closely located to PZ 2 samples in the ordination space, thus, indicating the proximity of the PZ 2 pollen assemblage to Interbed 1 respectively Interbed 2 pollen assemblages (Fig 5C, resp. 6C).

In contrast to PZ 1, dinoflagellate cysts are completely missing in PZ 2. In the composition of the pollen assemblage the most striking change is the occurrence of *Alnipollenites verus* (Betulaceae, *Alnus,* Fig 8L), which reaches a maximum of 57.5% in section S2. Although much lower, the maxima of *A. verus*, too, occur in PZ 2: 25.3% in section N resp. 2.9% in section S1.

Tricolporopollenites cingulum (Fagaceae) is among the dominant elements in sections N and S2. In section S1 maximum values are distinctly lower, but also reached in PZ 2. Other taxa with maxima in PZ 2 are *Spinaepollis spinosus* (Euphorbiaceae?), *Nyssapollenites* spp. (Nyssaceae, Figs 8N, O) and *Ilexpollenites* spp. (Aquifoliaceae, Fig 8P). The lowest values for these taxa occur again in section S1. *Inaperturopollenites* sp. is still characterized by high values (24.6%), a slight decrease, however, from PZ 1.

A few taxa decrease strongly within PZ 2 and, therefore permit the separation of subzones PZ 2a and PZ 2b for sections N and S2. This is the case, in particular, for *Thomsonipollis magnificus* (unknown botanical affinity, Fig 9F) which drops from 18% in section N to near absence in PZ 2b. Similarly, the fern spores *Leiotriletes* spp. (Schizaeaceae, Figs 9B, C, D) and other trilete spores

disappear almost completely in PZ 2b except for a slight increase at the top of PZ 2 in section S1. These spores are replaced by in PZ 2b by other fern spores like *Laevigatosporites* spp. (Polypodiaceae, Fig 9 E), which are rare in PZ 2a.

Fig 9. Important palynomorphs of PZs 3 and 4. (A) *Tricolporopollenites belgicus,* unknown botanical affinity (sample S1-2), (B) *Leiotriletes microadriennis,* Schizaeaceae (sample S1-4), (C) *Leiotriletes adriennis,* Schizaeaceae (sample S1-6), (D) *Leiotriletes paramaximus,* Schizaeaceae (sample S1-4); (E) *Laevigatosporites discordatus,* Polypodiaceae (sample S1-3); (F) *Thomsonipollis magnificus,* unknown botanical affinity (sample S1-2); (G) *Milfordia incerta,* Restionaceae (sample S1-9); (H) *Basopollis atumescens,* unknown botanical affinity (sample S1-8); (I) *Triporopollenites crassus,* Myricaceae (sample S1-10), (J) *Triporopollenites robustus,* Myricaceae (sample S1-8), (K) *Triporopollenites rhenanus,* Myricaceae (sample S1-8), (L) *Pompeckjoidaepollenites subhercynicus,* unknown botanical affinity (sample S1-3), (M) *Ericipites ericius,* Ericaceae (sample S1-11); scale bars: 10µm

The relative loss of these taxa in PZ 2b is in part made up by increases in *Monocolpopollenites tranquillus* (Arecaceae, *Phoenix*), *Tricolpopollenites retiformis, Tricolporopollenites belgicus* (unknown botanical affinity, Fig 9A) and *Tricolpopollenites liblarensis* in section S2 (Fig 7A), in section N additionally by *Ilexpollenites* spp. (Fig 5A). The small number of samples in section S1 here precludes a subdivision of PZ 2.

Palynozone 3 (Seam 1)

PZ 3 covers the middle of Seam 1 and is represented by 4 samples each in sections N and S1 and by 3 samples in section S2. The NMDS of all sections show that samples of PZ 3 are separated from other PZs in the ordination space indicating a unique assemblage composition. Especially in

393 sections N and S2 (Fig 5C resp. 7C) the samples are plotted midway between those of PZ 2 and PZ
394 4 indicating that the assemblages include elements from the preceding and succeeding PZs. In
395 section S1 PZ 3 is plotted on the left side of the ordination space clearly separated from the other
396 two seam-related PZs (Fig 6C). However, sample S1-5 is plotted far away from the other samples
397 of PZ 3 on the negative end of NMDS axis 1 (Fig 6C) suggesting a difference in assemblage
398 composition not readily recognized in the pollen diagram (Fig 6A).

399 *Alnipollenites verus* has virtually disappeared except for local abundance in section S2.
400 Similarly, *Tricolporopollenites cingulum* drops from high values in section N to 10.8% and from
401 low values in section S1 to less than 1%. Only in section S2 it remains at similar high levels. Other
402 taxa such as *Spinaepollis spinosus*, *Ilexpollenites* spp., *Nyssapollenites* spp., and *Tricolpopollenites*
403 *liblarensis* decrease consistently in sections N and S1 as well as *Tricolporopollenites belgicus* in
404 section S2.

405 *Pompeckjoidaepollenites subhercynicus* (unknown botanical affinity, Fig 9L) suddenly
406 appears with high values (up to 20.2% in section S1) and extends to the base of PZ 4 in sections N
407 and S2. *Triporopollenites robustus* (Myricaceae, Figs 9I - K) as well as spores of Sphagnaceae
408 such as *Sphagnumsporites* sp., *Tripunctisporis* sp. and, *Distancorisporis* sp. [68] (Fig 10) are
409 abundant before becoming prevalent in PZ 4. Both, *T. robustus* and *Sphagnum*-type spores together
410 are already prevalent in PZ 3 of section S1.

411

412 **Fig 10. Variation of *Sphagnum*-type spores in PZs 3 and 4.** Morphological variation in
413 *Tripunctisporis* sp. (A), (B), *Sphagnumsporites* sp. (C) and *Distancorisporis* sp. (D), (E), (F); scale
414 bars: 10µm

415

Sample S1-5 (section S1) is exceptional among PZ 3 samples (Fig 6C) due to the high abundance of spores of ferns and peat mosses. More than two thirds of the palynomorphs in this sample are composed of spores. Accordingly, *P. subhercynicus* and *T. robustus* remain proportionally rare.

Palynozone 4 (Seam 1)

PZ 4 comprises the upper part of Seam 1 and represents a significant change from the palynomorph assemblages of preceeding PZs 2 and 3 (Figs 5A, 6A, 7A). This becomes particularly evident in the NMDS. In all three sections samples of PZ 4 are clearly separated from all other samples in the ordination space (Figs 5C, 6C, 7C) due to the dominance of *Sphagnum*-type spores, which reach now their maximum with values between 38% and 52%. A similar dominance is shown for myricaceous pollen, e.g., *Triporopollenites robustus/rhenanus,* with values between 23% and 30%.

Pompeckjoidaepollenites subhercynicus, a major element of PZ 3 continues with high values (up to 28%) into the lower part of PZ 4 in sections N and S2. In section S1, however, it is rare. Pollen of the Normapolles group (e.g. *Basopollis* spp., Fig 9H) and Restionaceae (*Milfordia* spp., Fig 9G) have a strong showing in PZ 4 of section S1, but together with *Ericipites* spp. (Ericaceae, Fig 9M) a distinct reduction over PZ 3 in section N. *Momipites punctatus* (Juglandaceae, *Engelhardia*) is quite common for the first time in section S2 but rare in the other two section. *Laevigatosporites* spp. are reduced in sections S1 and S2 but increase in section N. *Alnipollenites verus* has been virtually lost in PZ 4 of all sections.

Palynozone 5 (base Interbed 2)

PZ 5 includes mainly samples from Interbed 2 (Figs 5A, 6A, 7A). In all sections a marine influence is indicated by the onset of the dinocysts *Apectodinium* spp. with maximum values of 65.5%. This clearly distinguishes the transition of Interbed 1 to the seam from the transition of the top of the

seam to Interbed 2. However, the NMDS of sections N (Fig 5C) and S2 (Fig 7C) show that the palynomorph assemblage composition of both is similar at the beginning and end of seam development. Both PZs are plotted in the ordination space in close vicinity. The NMDS of section S1 (Fig 6C), however, shows similarities in assemblage composition between PZ 5 and PZ 2 since one of the samples (S1-12) is plotted in the NMDS in the upper right corner of the ordination space. However, according to the cluster analysis, the closest similarity of S-12 is to S1-1 at the base of the seam (Fig 6B).

Drastic changes from PZ 4 are the disappearance of *Sphagnum*-type spores and the strong increase of *Inaperturopollenites* spp. with a maximum of 41.3% in section S1. These are similar values as in PZ 1. The pollen of the juglandaceous alliance such as *Plicapollis pseudoexcelsus* (up to 4.8%) and *Plicatopollis* spp. (up to 8.9%) as well as the fagaceous pollen *Tricolpopollenites liblarensis* (up to 15.5%) reach also high values that are in the range of their values within PZ 1. *Triporopollenites robustus/rhenanus* (up to 9%) are also common, although the values strongly decrease compared to PZ 4.

Non pollen/spore palynofacies (section S2)

In section S2 a selection of organic particles, such as fungal remains, periderm cells, cuticle fragments, resin and tannin bodies (resinite/phlobaphinite) as well as charcoal have been quantitatively recorded in addition to palynomorphs and calculated to 100% palynomorphs (Fig 11).

Fig 11. Abundance of non-pollen/spore palynofacies elements (NPP) in section S2. Diagram of 30 samples from the top of Interbed 1 to the base of Interbed 2 of section S2 showing the

462 distribution of NPPs. The zonation of the diagram is based on unconstrained cluster analysis of
463 palynomorph taxa (see Fig 7).
464
465 Fungal remains are common in PZ 2, albeit with wide variations in frequency between
466 barely present and 28%. In PZ 3 and PZ 4 fungal values drop to a few percent (less than 6%) only
467 to rise at the very top of the seam again. As may be expected, fungal remains hardly stray beyond
468 the seam.
469 This holds true for periderm cells as well. However, contrary to fungal remains periderm
470 cells are nearly absent in the lower part of PZ 2 (PZ 2a) but rise markedly at the base of PZ 2b.
471 With sample S2a-10 they drop back to insignificance only to return, similar to fungal remains, near
472 the top of the seam with maximum values (18%). It is interesting that the marked change in
473 periderm cells from PZ 2a to PZ 2b is accompanied by an equally marked increase of some
474 tricol(po)rate taxa, e.g. *Tricolpopollenites retiformis, T. liblarensis/microhenrici* and
475 *Tricolporopollenites belgicus* (Fig 7A). Cuticle fragments are remnants of leaf cuticles which are
476 easily drifted out to sea and washed onshore along shoreline drift [69,70]. Accordingly, they appear
477 most frequently in PZ 1 and PZ 5.
478 Resin (resinite) and tannin-derived bodies (phlobaphinites) are the most common organic
479 components second to charcoal. They represent cell fillings set free from decaying wood and are
480 most abundant in PZ 2a and PZ 2b, but common to frequent throughout the whole seam with
481 considerable fluctuation.
482 Charcoal particles become the dominant non-palynomorph element in PZ 3 and especially
483 in PZ 4 in striking parallelism to the frequency of *Sphagnum*-type spores and the *Triporopollenites*
484 *robustus/rhenanus* group. The appearance of pollen of the Normapolles group and freshwater algae
485 (Zygnemataceae) also coincides with the dominance of charcoal in PZ 4.

Diversity (section S1)

In order to get estimates for palynological richness, rarefaction analyzes of 11 samples from Seam 1 were performed, distinguishing between point diversity within a single sample (Fig 12A, Table 1), alpha diversity within PZs 2 to 4 (Fig 12B, Table 2) and gamma diversity for the entire seam (Fig 12C, Table 2). Furthermore, analysis of beta diversity as well as evenness have been carried out (Tables 1, 2).

Fig 12. Palynological richness calculations for Seam 1 in section S1 using rarefaction analyses. (A) Point diversity: Individual rarefaction with conditional variance of 11 samples of Seam 1 using the algorithm of [71]. (B) Alpha diversity: Sample-based interpolation and extrapolation using the Bernoulli product model [56] for the 3 palynozones (PZ) of Seam 1 with 95% unconditional confidence intervals; Sobs, number of observed species. (C) Gamma diversity: Sample-based interpolation and extrapolation using the Bernoulli product model [56] for the entire data set of samples from Seam 1; Sobs, number of observed species. Because of differences in the number of counted individuals per sample, the sample-based rarefaction curves and their confidence intervals in (B) and (C) are replotted against an x-axis of individual abundance.

509 **Table 1: Estimations of palynological richness and evenness based on individual rarefaction**

510 **analysis for 11 lignite samples of section S1 (point diversity).**

	S1-1	S1-2	S1-3	S1-4	S1-5	S1-6	S1-7	S1-8	S1-9	S1-10	S1-11
Individuals counted	416	346	343	502	305	316	304	316	310	329	328
S_{obs}	74	88	63	59	30	41	48	45	50	51	72
$S(est)_{300}$	61.7	81.6	58.6	46.3	29.7	40.0	47.8	43.8	49.3	48.3	68.2
$S(est)_{300}$ Std.err, 2σ, Lower Bound	56.1	77.3	54.9	40.8	28.7	38.1	46.8	41.7	47.7	45.3	64.7
$S(est)_{300}$ Std.err, 2σ , Upper Bound	67.4	86.0	62.3	51.7	30.8	41.9	48.7	45.9	50.9	51.3	71.7
Shannon-Wiener index	3.24	3.70	3.13	2.84	2.19	2.76	3.13	2.72	3.02	2.37	3.19
Eveness (E)	0.79	0.84	0.77	0.74	0.65	0.75	0.81	0.72	0.78	0.61	0.76

511 S_{obs}: Actual number of taxa within the samples; $S(est)_{300}$: Expected number of species for 300
512 counted palynomorphs using the algorithm of [71]; $S(est)_{300}$ Std.err, 2σ: Lower and upper bounds
513 for a standard error of two-sigma of unconditional variance for 300 palynomorphs; evenness
514 calculation using the method of [58]: E = Shannon-Winter index/ln(S_{obs}).

515

516 **Table 2: Estimations of richness and evenness using sample-based incidence data for the 3**

517 **palynozones (PZ) of Seam 1 (alpha diversity) and for all samples of Seam 1 (gamma diversity).**

	PZ 2	PZ 3	PZ 4	Seam 1
Number of samples (n)	3	4	4	11
S_{obs}	126	99	110	179
Individuals counted	1105	1427	1283	3815
$S(est)_5$	144	111	119	217*
$S(est)_5$ 95% CI, Lower Bound	131.2	96.5	107.9	196.0*
$S(est)_5$ 95% CI, Upper Bound	154.7	124.6	130.5	238.3*
Singeltons	49	40	41	58
Doubletons	21	13	21	20
Shannon-Wiener index	3.89	3.09	3.12	3.69
Eveness (E)	0.80	0.67	0.66	0.71
Beta diversity	0.68	1.23 (0.74**)	1.02	2.17

518 S_{obs}: Actual number of taxa within the samples; $S(est)_5$: Expected number of species in 5 samples
519 using the Bernoulli product model [56]; $S(est)_5$ 95% CI: Lower and upper bounds of 95%

520 confidence interval for S(est); *S(est) and *S(est) 95% CI in 20 samples; Singletons: Number of
521 species that occur only once in all samples; Doubletons: Number of species that occur only twice
522 in all samples; evenness calculation using the method of [58]: E = Shannon-Winter index/ln(S_{obs});
523 beta diversity using the measure of [59,64]: (S/ā) – 1 (S, total number of species in the PZ or Seam
524 1; ā, average number of species in the PZ or Seam 1; ** beta diversity estimation without sample
525 S1-5).
526
527 Comparing point diversity within the seam as based on individual rarefaction analyzes
528 using the algorithm of [71], samples of PZ 2 (S1-1 to S1-3) together with sample S1-11 from the
529 top of the seam provide the highest richness values (Fig 12A). While in samples S1-1, S1-3 and
530 S1-11 between 59 and 68 species at 300 counted individuals can be expected, sample S1-2 shows
531 by far the highest number with 82 species (Table 1). The richness in samples from the succeeding
532 PZs 3 and 4 (samples S1-4 to S1-10) is significantly lower with values typically ranging from 40
533 to 49 species among 300 counted palynomorphs (Table 1). In sample S1-5, which differs distinctly
534 in composition of the microflora from the other samples of Seam 1 in the section (Fig 6C), even a
535 much lower value with only 30 different species is achieved. Therefore, a decrease in palynological
536 richness between PZ 2 and PZs 3 and 4 is obvious. Only at the top of the seam in sample S1-11 an
537 increase of richness to values similar to those in PZ 2 is recognizable.
538 The same pattern of species richness is also evident in alpha diversity (Fig 12B). 126
539 different pollen and spore taxa have been recorded in the three samples of PZ 2, while significantly
540 lower numbers were observed in the subsequent PZ 3 with 99 species and in PZ 4 with 110 species,
541 although the number of samples and of counted palynomorphs in these two PZs is higher than in
542 PZ 2 (Table 2). Even if the 95% confidence intervals are considered, which describe the range of
543 the possible number of species within the PZs, the richness in PZ 2 is significantly higher than in

the two subsequent PZs (Table 2). For PZ 3 and PZ 4 the 95% confidence intervals overlap somewhat (Fig 12B). A diversity increase from PZ 3 to PZ 4 is therefore indicated by the richness estimations, but it is not statistically significant. Furthermore, the interpolation/extrapolation graph of PZ 3 is not saturated indicating that the maximum number of species is higher than calculated and may possibly be in the same range or even higher than in PZ 4.

The high number of singletons and doubletons, showing the number of species with only one or two individuals within the data set, is striking (Table 2). For example, 70 of 126 species of pollen and spores in PZ 2 and 53 of 99 species in PZ 4 have only been recorded one or two times. Therefore, *c*. 55% of the species in the three PZs are singletons or doubletons indicating accordingly that more than half of the species within the total pollen assemblages belong to rare taxa.

The analysis of gamma diversity (Fig 12C) shows a high overall species richness for the entire section. 179 different species have been detected in Seam 1. An extrapolation to 20 samples even indicates a much higher number of morphologically distinct species (217, see Table 2). Since the interpolation/extrapolation graph is not saturated, even more species can be expected (Fig 12C).

Beta diversity as a measure of the difference in species composition is especially high in comparison between sample S1-5 and the other samples with values always higher than 0.6 (S5 Table). This underlines the special composition of the palynomorph assemblage of sample S1-5 in comparison to the other lignite samples of section S1. In contrast, the values for beta diversity of sample comparisons within the same PZs are generally below 0.5 or between 0.5 and 0.6 if samples of different PZs are compared. This indicates minor changes in the composition of the palynomorph assemblages within the PZs, but changes in composition between PZs 2, 3, and 4. This is also confirmed by general beta diversity calculations for the PZs (Table 2). They are low with 0.68 for PZ 2 and 1.02 for PZ 4. Only in PZ 3 the value increases to 1.23, but this is again due to the specific

568 composition of the palynomorph assemblage in sample S1-5. If this sample is excluded from the
569 analysis, the value drops to 0.74. In contrast, the total beta diversity value for Seam 1 is significantly
570 higher with 2.17, indicating strong changes in the composition of the palynomorph assemblages
571 between the individual PZs (Table 2).

572 In addition to species richness, the calculation of evenness provides another important
573 parameter for diversity analysis. In single samples from Seam 1, usually evenness values of more
574 than 0.7 are reached (Table 1). These high values show that the different palynomorph species
575 within the microfloral assemblages are distributed relatively evenly in the individual samples in
576 general. This indicates that (except for the high number of rare elements which contribute to the
577 richness calculation) none of the abundant elements is clearly dominating. Only in samples S1-5
578 and S1-10 the evenness values decrease to 0.64 and 0.61 showing that in these samples a dominance
579 of some elements within the pollen assemblage becomes apparent.

580 PZ 3 and PZ 4 are characterized by relatively low evenness values of 0.67 and 0.66 (Table
581 2). In contrast, the evenness for PZ 2 is significantly higher with 0.8. Together with the high value
582 for species richness, the high evenness value therefore proves a morpho-diversity in samples of PZ
583 2 that is significantly higher than in PZ 3 and PZ 4. The evenness value of 0.71 for the entire seam
584 is in accordance to the values of the individual samples (Table 2).

585

586 Discussion

587 Reconstruction of the paleoenvironment

588 The NMDS of all three sections show a distinctive threefold succession of vegetation during
589 formation of Seam 1 (Figs 5, 6, 7): an initial (PZ 2), a transitional (PZ 3) and a terminal stage (PZ

590 4). Such tripartite divisions appear to be common in coastal plain (paralic) coals and have been
591 described and interpreted in terms of environment and vegetation first from the Carboniferous of
592 Britain [72-74]. Mechanisms controlling facies and environment during transgression and
593 regression in peat forming paralic domains have recently been reviewed by [75]. Seam 1 is
594 sandwiched between Interbeds I (PZ 1) and II (PZ 5), both showing marine influence and being
595 largely separated from the PZs 2 to 4 in the NMDS of the total data set (Fig 13). Thus in total the
596 following four different types of paleoenvironment and vegetation can be distinguished in the three
597 sections: (1) a near coastal vegetation (PZ 1 and PZ 5), (2) a lowland mire (PZ 2), (3) a transitional
598 mire (PZ 3) and (4) a terminal mire (PZ 4). They are unaffected by the onset of a warming event
599 close to the top of the seam [13] and may therefore be considered as representing plant associations
600 typical for individual types of vegetation during the Early Eocene climatic background.

601

602 **Fig 13. Non-metric multidimensional scaling (NMDS) scatter plots of 56 samples from**
603 **sections N, S1 and S2.** (A) Arrangement of samples (B) Arrangement of palynomorph taxa. For
604 calculation the Bray-Curtis dissimilarity and Wisconsin double standardized raw-data values have
605 been used.

606

607 Near-coastal vegetation (PZ 1, PZ 5)

608 Sandwiched between two marine-influenced interbeds Seam 1 was deposited between a regressive
609 phase represented by PZ 1 (top of Interbed 1) and a transgressive phase represented by PZ 5 (base
610 of Interbed 2). The NMDS of the total data set (Fig 13A) shows that samples of PZ 1 and PZ 5 are
611 largely separated from most of the samples of Seam 1 in the ordination space but plot together with

612 some samples of PZ 2. This indicates that both marine influenced PZs include elements of the peat-
613 forming lowland mire vegetation in the background.

614 The dominance of *Inaperturopollenites* spp. in PZ 1 and PZ 5 shows that Cupressaceae s.l.
615 played an important role in the coastal vegetation. Together with *Nyssapollenites*, fairly common
616 in the succeeding PZ 2, they indicate that a *Nyssa/Taxodium* swamp forest existed adjacent to the
617 coast at Schöningen (Figs 13B, 14). Such a swamp community was originally reconstructed for the
618 Miocene Lower Rhine Lignite but the model has later been extended to examples from other areas
619 and Cenozoic ages [76,77]. Associated elements are *Plicatopollis* spp., *Tricolporopollenites*
620 *liblarensis* and *Plicapollis pseudoexcelsus*. The latter has been interpreted as a back-mangrove
621 element associated with marsh elements in the Middle Eocene Helmstedt Formation [10,78,79].
622 The anemophilous *Plicatopollis* spp. and *T. liblarensis* as well as the very thin-walled
623 *Inaperturopollenites* spp. are also likely to be derived from nearby external sources such as the
624 background mire forest (Fig 14 A).

625

626 **Fig 14. Paleoenvironment reconstruction for Seam 1.** Four different types of paleoenvironment
627 and vegetation can be distinguished in the three sections N, S1 and S2: (A) a near coastal vegetation
628 (PZ 1 and PZ 5) (B) a lowland mire (PZ 2) (C) a transitional mire (PZ 3) (D) a terminal mire (PZ
629 4).

630

631 Except for scattered occurrences of putative *Rhizophora* (Fig 14A) true mangrove pollen
632 characterizing the coastal vegetation of the middle Eocene Helmstedt Formation, such as *Avicennia*
633 and *Nypa* [10-12,78], is completely missing in the Schöningen Formation [11,13]. Instead,
634 *Pistillipollenites mcgregorii* and *Thomsonipollis magnificus* (both of unknown botanical affinity)
635 may have substituted there for mangrove elements [11]. Since *T. magnificus* occurs regularly in PZ

1 and 5 in sections S1 and S2 and is very abundant in PZ 2a in section N, where *P. mcgregorii* also occurs at least in low numbers, the parent plants of both taxa were probably common in the immediate coastal vegetation during the deposition of the lower part of the Schöningen Formation.

Finally, cuticle fragments which are abundant in both, PZ 1 and PZ 5, may have had their source in the near-coastal vegetation and were concentrated along the shoreline by winnowing [69,70].

Lowland mire (PZ 2)

At the onset of Seam 1 palynomorph assemblages combined in PZ 2 indicate a trend in the vegetation that started in PZ 1 and pass into PZ 3. As shown by the NMDS samples of PZ 2 are plotted together on the negative side of axis 1 in the ordination space (Fig 13A). However, there is only little separation from the samples of PZ 1 and PZ 5 and an overlap with samples from the following PZ 3.

The abundance of *Inaperturopollenites* spp. (Cupressaceae s.l.) and the common occurrence of *Nyssapollenites* spp. (Nyssaceae) on either side of the interbed/seam boundary support the existence of a *Nyssa/Taxodium* swamp forest in the immediate vicinity of the coastline. This swamp forest may have been locally replaced by or mixed with patches of other elements, such as the mother plant of *Plicapollis pseudoexcelsus* (base of PZ 2 in section N and S1, Figs 5, 6), a characteristic element of transitional marine/terrestrial environments of possible juglandaceous affinity [10,78,79]. *Thomsonipollenites magnificus* is quite abundant in section N (PZ 2a) in contrast to the other two sections.

In particular, *Alnipollenites verus* (*Alnus*) is common to frequent throughout PZ 2 and even highly dominant in some samples of section N (e.g., N4, Fig 5) and S2 (e.g., S2-a2, Fig 7). For these sites freshwater wetland habitats may be envisioned similar to those in which modern species of *Alnus* such as e.g. *A. glutinosa* [80], *A. incana* [81] or *A. viridis* [82] grow today. Intermittent

660 open fern meadows are indicated by the strong proliferation of trilete spores at the base of PZ 2 in
661 section N. Notably, these spores are absent in the other two sections. Other common associates of
662 PZ 2 assemblages such as *Monocolpopollenites tranquillus* (Arecaceae, *Phoenix*), *Plicatopollis*
663 spp., and *Tricolpopollenites liblarensis* may have been in part indigenous to PZ 2, but they are
664 small and thin-walled, therefore considered to be anemophilous [24] and likely to be introduced
665 from other sources.

666 Local differences shown in the three sections are a special feature of PZ 2 indicating a
667 pronounced patchiness in the lowland vegetation (Fig 14B). These variations in species
668 composition and dominance at the initiation of Seam 1 are associated with local changes in water
669 tables and nutrient levels as well as exposure to the sea (salinity) as shown by successional changes
670 in modern taxodiaceous and tropical angiosperm swamp forests [83-86].

671 This is also reflected in the striking contrast between subzones PZ 2a and PZ 2b in sections
672 N and S2. Notable is, for instance, the replacement of fern spores (*Leiotriletes* spp.) in section S2
673 by pollen of woody plants such as *Tricolporopollenites belgicus* (Fig 7). The apparent change from
674 a herbaceous vegetation rich in ferns in PZ 2a to a more woody vegetation in PZ 2b is even reflected
675 in the distribution of non-palynomorph organic remains showing an increase of periderm cells,
676 phlobaphinites and resin particles as well as fungal remains from PZ 2a to PZ 2b (Fig 11).

677 Transitional mire (PZ 3)

678 The change in vegetation occurring within PZ 3 is gradual. Previously dominant elements such as
679 *Alnus* (*Alnipollenites verus*) or the Cupressaceae s.l. (*Inaperturopollenites* spp.) are replaced by
680 taxa such as *Pompeckjoidaepollenites subhercynicus,* pollen of the *Triporopollenites*
681 *robustus/rhenanus* group as well as *Sphagnum*-type spores the latter two of which become
682 eventually dominant in the succeeding PZ 4.

683 Accordingly, the samples of PZ 3 plot midway between those of the clearly separated PZ 2
684 and PZ 4 in the ordination space of the NMDS of the total data set (Fig 13A). There are, however,
685 considerable areas of overlap with both PZs which characterizes PZ 3 as transitional between the
686 initial and the terminal phases in the formation of Seam 1. The PZ 3 samples of section S2 differ
687 from those of the other two sections since they plot separate to the left on the negative side of axis
688 1 (Fig 13A). This is due to the fact that the similarity of samples from S2 to those of PZ 2 is closer
689 than in the other two sections, which are more transitional to PZ 4.

690 *P. subhercynicus* (unknown botanical affinity) and the *T. robustus/rhenanus* group pollen
691 (Myricaceae) are widely distributed throughout the Schöningen Formation and often dominant in
692 the upper part of the lower seams (Main Seam, Seam 1 and Seam 2 [13]). *P. subhercynicus* is more
693 restricted to certain levels and appears to prefer mire forest/marsh interfaces (ecotones) [10,12].
694 The *T. robustus/rhenanus* group is locally abundant in PZ 3 and even dominant in section N before
695 becoming dominant throughout PZ 4. Noteworthy is the first strong appearance of *Sphagnum*-type
696 spores indicating an initial tendency for ombrogenous bogs to develop under an open canopy of an
697 angiosperm mire forest (Fig 14C).

698 Sample 5 of section S1 is clearly separated from all other samples in the NMDS (Fig 6C,
699 Fig 13) due to the dominance of peat moss and fern spores (*Sphagnum*-type spores,
700 *Laevigatosporites* spp., *Leiotriletes* spp.) coinciding with a mass occurrence of charcoal particles.
701 The sample was taken from a tree stump layer (X-Horizon) suggesting that a tree throw or fire may
702 have left a clearing allowing ferns and mosses to settle as pioneering elements.

703

704 Terminal mire vegetation (PZ 4)

705 A very marked change in palynomorph assemblage composition occurs at the transition from PZ 3
706 to PZ 4. This is mainly due to the rise to dominance of *Sphagnum*-type spores including all three

707 genera previously observed in seams of the Schöningen Formation, i.e. *Sphagnumsporites,*
708 *Tripunctisporis* and *Distancorisporis* [27,68]. Although the latter two are morphologically
709 different from modern *Sphagnum* spores the three genera are sufficiently similar and closely
710 associated with remains of *Sphagnum* leaves in a thin lignite seam (*Sphagnum* Seam) higher up in
711 the Schöningen section to confirm their affinity to *Sphagnum* [11,27,68].

712 The change in PZ 4 is underscored by the great increase in pollen of the *T.*
713 *robustus/rhenanus* group. Although some of these changes are already initiated in section N (for
714 *T. robustus/rhenanus*) and section S1 (for *Sphagnum*-type spores), the NMDS of all three sections
715 (Figs 5C, 6C, 7C) and of the total data set (Fig 13A) show a clear separation of PZ 4 samples from
716 those of all other PZs.

717 According to SEM studies of the authors (VW and WR, unpublished) *T. robustus* should
718 be considered as derived from Myricaceae, a family today represented by small trees and shrubs
719 adapted to wet acidic environments and nutrient deficiency [87,88]. Together with *Sphagnum* they
720 clearly signal that peatbeds in PZ 4 were decoupled from groundwater and their hydrology
721 increasingly controlled by precipitation [89-91] (Fig 14D). The increase of *Ericipites* sp. (Ericaceae)
722 and *Milfordia* spp. (Restionaceae) in section S1 is fully in line with this development. In particular,
723 Restionaceae have been described as an important constituent of the so-called *Sphagnum* Seam at
724 Schöningen which has been compared with a southern hemisphere restionad bog [27]. At least
725 temporarily standing water is indicated by the rare but regular occurrence of remains of freshwater
726 algae such as spores of Zygnemataceae (Fig 14D).

727 Somewhat intriguing are certain members of the Normapolles such as *Basopollis* and
728 *Nudopollis*, relics from the Cretaceous, the occurrence of which is one of the last in the Paleogene
729 of Central Europe and largely restricted here to PZ 4. Their parent plants seem to have found refuge
730 within the vegetation and environment of PZ 4 just prior to their extinction. However, the

731 association of *B. orthobasalis* with pollen of plants that are adapted to nitrogen and phosphorus
732 deficient substrates such as Myricaceae in the Paleocene show that they also favored nutrient poor
733 substrates [94].

734 The multiple evidence of waterlogged conditions and standing water, however, seems
735 counterintuitive to the massive occurrence of charcoal particles (Fig 11) some of which show
736 pitting and are, therefore, wood derived. This apparent contradiction may be resolved in three ways:
737 by close lateral proximity of burnt and waterlogged to aquatic sites, by crown fires in a temporarily
738 flooded mire forest or by periodic drought followed by flooding and resettlement of burned forest
739 sites. A possible modern equivalent for the latter may be provided by the complex fire regime in
740 the Okefenokee Swamp (Georgia, USA) [95], where periodic forest fires at approximately 25 year
741 intervals left charcoal horizons, but also maintained open areas, the so-called wet prairies which
742 include peat mosses [96,97]. New peat was deposited after each fire [98]. In PZ 4 of Seam 1 new
743 peat was formed among others by regrowth of *Sphagnum*, ferns, Restionaceae (section S1), and
744 shrubs (Myricaceae, Betulaceae, Juglandaceae).
745

746 Diversity

747 The study of the morpho-diversity of the pollen assemblages in section S1 allows for an estimate
748 of the diversity of the vegetation, assuming that the pollen rain reflects relative changes within the
749 vegetation [58,61]. 179 palynomorph species have been recognized in Seam 1, but gamma diversity
750 calculation shows that more than 200 species can be expected (Fig 12C, Table 2). Thus, the
751 diversity is distinctly higher than calculated for other Lower Eocene records, especially those in
752 North America (Mississippi, Alabama) [99,100]. However, the calculations may be based on
753 different taxonomic resolution and should be considered with caution. In any case, the diversity

754 measures of Seam 1 reflect a high plant diversity as typical for forested tropical coastal wet- and
755 peatlands [101].

756 The high morpho-diversity of the microflora in PZ 2 is striking. The point diversity of
757 samples S-1, S-2, and S-3 of section S1 and the alpha diversity are significantly higher than in the
758 other samples or PZs in S1 (Figs 12A, B). This may be related to the fact that PZ 2 represents a
759 mixture of elements from the coastal vegetation and the subsequent lowland mire forest. However,
760 a lowland mire forest, as represented in PZ 2 is in any case highly diverse compared to a disturbed
761 terminal mire vegetation with raised bog that follows later [101].

762 With the initiation of a *Sphagnum* bog a peat swamp developed that became increasingly
763 oligotrophic supporting plant communities that are adapted to low pH and nutrient depletion and
764 low in diversity [102]. Accordingly, the samples of PZ 3 as well as the samples of the lower part
765 of PZ 4 are characterized by the lowest point diversity (Fig 12A). Alpha diversity of PZ 3 is also
766 significantly lower than in PZ 2 (Fig 12B).

767 In the uppermost sample of PZ 3 the point diversity clearly increases again (Fig 12A) since
768 immediately prior to the transgression of Interbed 2 species-rich back swamp and coastal
769 communities returned to the site. Sample S1-5 (X-horizon) clearly differs from all other samples
770 of Seam 1 because point diversity and evenness are by far the lowest due to the dominance of
771 spores and the concomitant decline of other elements (Fig 12A, Table 1). Possibly, a temporary
772 clearing in the mire forest may have been settled there by ferns and mosses as pioneer elements.

773

774 Paleoclimate

775 Isotope analyses have recently shown that a Carbon isotope excursion (CIE) indicates a short-term
776 thermal event that started at the topmost sample of Seam 1 extending into the lower part of Seam
777 2 [13]. Nevertheless, the bulk of Seam 1 was deposited during a moderately warm period of the

778 Lower Eocene as suggested below. However, temperature reconstructions for Seam 1 based on
779 biomarker analysis (brGDGTs) resulted in high mean annual temperatures (MAT), which reached
780 24°C ± 4.6°C in the lower part of the seam [103]. Therefore, a thermophilic vegetation should be
781 expected similar to other sites along the southern coast of the Proto-North Sea such as Cobham
782 (southern England) and Vasterival (France) which included the PETM [104,105].

783 We present evidence here that the vegetation of Seam 1 indicates a cooler mesothermal
784 climate. True humid tropical mangrove elements such as *Avicennia* and *Nypa*, common in the
785 coastal vegetation of the succeeding Middle Eocene Helmstedt Formation [10,78], are absent. This
786 suggests at least extratropical conditions for the Schöningen Formation [11]. On the other hand,
787 *Alnus*, one of the characteristic elements of PZ 2 does not occur in the PETM records of the Cobham
788 lignite and Vasterival [104,105]. The assemblages of PZ 2 are more compatible with high-latitude
789 Eocene swamp forests such as those on Axel Heidberg Island in the Canadian High Arctic, where
790 Cupressaceae s.l. and *Alnus* are widely distributed [106]. A similar microflora is also known from
791 the Paleocene/Eocene boundary in the central North Sea [107], where the vegetation is composed
792 of mesothermal conifers (Cupressaceae s.l.) and dicots such as *Alnus*, *Carya* and *Juglans* indicating
793 a mixed conifer broadleaf vegetation [107]. Temperature reconstructions for this record based on
794 comparisons with nearest living relatives (NLR) indicate relatively cool mean annual temperatures
795 (MAT) of 15° C and cold month mean temperatures (CMMT) of 8° C but warm month mean
796 temperatures (WMMT) of 22.5° C for the North Sea region [107]. The similarly composed
797 palynomorph assemblages of PZ 2, in particular the high abundance of *Alnus* pollen, would,
798 therefore, suggest similar extratropical conditions for Seam 1. This is a considerably cooler
799 estimate than that based on biomarker analysis notwithstanding the resemblance of WMMT
800 estimates. However, this may be explained by the fact that a certain temperature bias between
801 brGDGTs estimates and those from leaves and palynomorphs is well known [107,108].

Although *Alnus* as a temperate climate element declines in PZ 2 and PZ 3 extratropical conditions seem to have persisted through PZ 3 and PZ 4 since *Sphagnum* and fern spores in association with pollen of Restionaceae and Ericaceae dominate [11,27]. They are typical for temperate mires in the southern hemisphere today. In the northern hemisphere similar pollen assemblages are also known from Paleocene to Lower Eocene coals of Texas and Wyoming [109].

The close association of *Sphagnum* and fern spores with high abundances of charcoal in PZ 3 and PZ 4 (Fig 11) appears rather contradictory and has been interpreted in a number of ways also with regard to climate. In any case, the great increase in charcoal points to an increase in fire activity and possibly to dryer conditions in the area toward the end of Seam 1 formation. [68] argued that wildfires impeded the spread of taller and more vulnerable vascular plants and thereby advanced the spread of *Sphagnum*. On the other hand, the highest abundance of charcoal at the top of PZ 4 (Fig 11) may be correlated with the onset of a CIE [13] considering that an increase of wildfires shortly before the onset of the PETM has been noted for the Cobham lignite [104,110]. This could give support to the suggestion that peat burning may have been a trigger for CIEs and associated thermal events in the early Paleogene [111,112]. However, we favor the Okefenokee Swamp (Georgia, USA) as a recent example for conditions existing during PZ 4, in which periodic droughts and subsequent forest fires under a warm-temperate climate leave open areas later invaded by a herbaceous vegetation consisting of *Sphagnum*, ferns, Restionaceae and Ericaceae with aquatic sites in between.

Conclusions

Statistical scrutiny by means of Cluster analyses and NMDS shows that 5 different PZs occurring in vertical succession can be clearly distinguished in the three sections of Seam 1 despite local differences between them. They reflect vegetation responses to changes in environment and facies

that take place during an early Paleogene regression/transgression cycle including the formation of a coal seam. The two PZs bounding the seam, PZ 1 and PZ 5, are similar mainly due to the presence of marine indicators (*Apectodinium*, *Rhizophora*) and reflect the state of vegetation during the regressional respectively transgressional phase. PZ 2 to PZ 4 represent changes occurring during seam formation. The initial phase (PZ 2) is characterized by a patchy, pioneering vegetation (e.g. *Thomsonipollis magnificus*, *Alnipollenites verus*) controlled by variable edaphic conditions. PZ 3 appears transitional in a seam of limited thickness, but represents a certain climax in mire development since it is composed of a mix of species adapted to these conditions. External factors increasingly lead to disturbances of the environment and extreme conditions for peat development supporting a rather heterogeneous vegetation of *Sphagnum*, ferns, and Myricaceae in combination with frequent charcoal (PZ 4) during the terminal phase.

Diversity measurements show that PZ 2 has the greatest species diversity as is commonly the case in ecotones containing elements from adjacent communities as well as specialists of different habitats. Since they disappear with progressive stabilization of the mire environment, diversity drops to the lowest in PZ 3, before disturbances of the environment create new habitats in PZ 4. This pattern may be considered typical of vegetation responses in regression/transgression cycles.

Climatic signals for Seam 1 are somewhat contradictory. Warm temperatures of ca. 24 °C have been calculated by biomarker analyses of Seam 1 approaching those accepted for the PETM [103]. Isotope analyses [13], on the other hand, have shown that Seam 1 has been formed just prior to a negative CIE excursion. There is strong palynological evidence from Seam 1 that a temperate climate prevailed in northwestern Germany during the lowermost lower Eocene, since *Alnus* and *Sphagnum* are abundant temperate elements in Seam 1, while tropical elements, e.g. *Avicennia*, *Nypa* and *Sapotaceae*, well known from the Middle Eocene Helmstedt Formation, are entirely

849 missing. Seam 1, therefore, stands as an example typical for the climate during the Early Eocene
850 apart from any thermal event. Thus, a complete isotope record and critical taxonomic inventory of
851 the palynology appears prerequisite to characterize any of the Early Eocene thermal events that
852 may occur above or below Seam 1.
853

854 Acknowledgements and funding

855 Olaf Lenz acknowledges support through a grant of the Deutsche Forschungsgemeinschaft (DFG
856 LE 2376/4-1). We thank Karin Schmidt for valuable field support and technical assistance. We are
857 also grateful to the MIBRAG (formerly BKB and later EoN) for access to the sections and technical
858 support in the field. We thank ## referees for their reviews and comments that helped to
859 significantly improve this paper.
860

861 References

862 1. Zachos JC, Pagani M, Sloan L, Thomas E, Billups K. Trends, rhythms, and aberrations in global
863 climate 65 Ma to present. Science. 2001; 292: 686 – 693.
864 2. Kennet JP, Stott LD. Abrupt deep-sea warming, palaeoceanographic changes and benthic
865 extinctions at the end of the Palaeocene. Nature. 1991; 353: 225–229.
866 3. Bains S, Norris RD, Corfield RM, Faul KL. Termination of global warmth at the
867 Palaeocene/Eocene boundary through productivity feedback. Nature. 2000; 407: 171–174.
868 4. Röhl U, Bralower TJ, Norris RD, Wefer G. New chronology for the late Paleocene thermal
869 maximum and its environmental implications. Geology. 2000; 28: 927–930.

5. Röhl U, Westerhold T, Bralower TJ, Zachos JC. On the duration of the Paleocene-Eocene thermal maximum (PETM). Geochemistry, Geophysics, Geosystems. 2007; 8: Q12002. doi:10.1029/2007GC001784, 2007.

6. Lourens LJ, Sluijs A, Kroon D, Zachos JC, Thomas E, et al. Astronomical pacing of late Palaeocene to early Eocene global warming events. Nature. 2005; 235: 1083–1087.

7. Sluijs A, Schouten S, Donders T., Schoon PL, Röhl U, Reichart GJ, et al. Warm and wet conditions in the Arctic region during Eocene Thermal Maximum 2. Nature Geiosciences. 2009; 2: 777–780.

8. Cramer BS, Wright JD, Kent DV, Aubry MP. Orbital climate forcing of δ13C excursions in the late Paleocene–early Eocene (chrons C24n-C25n). Paleoceanography. 2003; 18: 1097. doi: 10.1029/2003PA000909.

9. Röhl U, Westerhold T, Monechi S, Thomas E, Zachos JC, Donner B. The Third and Final Early Eocene Thermal Maximum: Characteristics, Timing and Mechanisms of the "X" Event. Geological Society of America, Abstracts with Programs. 2005; 37: 264.

10. Lenz OK. Palynologie und Paläoökologie eines Küstenmoores aus dem Mittleren Eozän Mitteleuropas-Die Wulfersdorfer Flözgruppe aus dem Tagebau Helmstedt, Niedersachsen, Palaeontographica B. 2005; 271: 1-157.

11. Riegel W, Wilde V, Lenz OK. The Early Eocene of Schöningen (N-Germany) – an interim report. Austrian Journal of Earth Sciences. 2012; 105: 88–109.

12. Riegel W, Lenz OK, Wilde V. From open estuary to meandering river in a greenhouse world – An ecological case study from the Middle Eocene of Helmstedt, northern Germany. Palaios. 2015; 30: 304-326.

13. Methner K, Lenz OK, Riegel W, Wilde V, Mulch A. Paleoenvironmental response of midlatitudinal wetlands to Paleocene–early Eocene climate change (Schöningen lignite deposits, Germany). Climate of the Past: 2019; 15: 1741-1755.

14. Brandes C, Pollok L, Schmidt C, Wilde V, Winsemann J. Basin modelling of a lignite-bearing salt rim syncline: insights into rim syncline evolution and salt diapirism in NW Germany. Basin Research. 2012; 24: doi: 10.1111/j.1365-2117.2012.00544x.

15. Blumenstengel H, Krutzsch, W. Tertiär. In: Bachmann GH, Ehling BC, Eichner R, Schwab M, editors. Geologie von Sachsen-Anhalt. Schweizerbart, Stuttgart; 2008. pp. 267-273.

16. Standke G. Paläogeografie des älteren Tertiärs (Paleozän bis Untermiozän) im mitteldeutschen Raum. Zeitschrift der Deutschen Gesellschaft für Geowissenschaften. 2008, 159: 81-103.

17. Wilde V, Riegel W, Lenz OK. Das Paläogen im Helmstedter Revier: Ein Forschungsthema im Geopark Harz. Braunschweiger Land. Ostfalen. Gaussiana. 2020; 1: Forthcoming.

18. Manger G. Der Zusammenhang von Salztektonik und Braunkohlenbildung bei der Entstehung der Helmstedter Braunkohlenlagerstätten. Mitteilungen aus dem Geologischen Staatsinstitut in Hamburg. 1952; 21: 7-45.

19. Gramann F, Harre W, Kreuzer H, Look ER, Mattiat B. K-Ar ages of Eocene to Oligocene glauconitic sands from Helmstedt and Lehrte (Northwestern Germany). Newsletter on Stratigraphy. 1975; 4: 71-86.

20. Gürs K. Das Tertiär Nordwestdeutschlands in der Stratigraphischen Tabelle von Deutschland 2002. Newsletters on Stratigraphy. 2005; 41: 313-322.

21. Ahrendt H, Köthe A, Lietzow A, Marheine D, Ritzkowski S. Lithostratigraphie, Biostratigraphie und radiometrische Datierung des Unter-Eozäns von Helmstedt (SE-Niedersachsen). Zeitschrift der Deutschen Geologischen Gesellschaft. 1995; 146: 450-457.

916 22. Köthe A. Dinozysten-Zonierung im Tertiär Norddeutschlands. Revue de Paléobiologie.
917 2003; 22: 895-923.
918 23. Pflug HD. Palynologie und Stratigraphie der eozänen Braunkohlen von Helmstedt.
919 Paläontologische Zeitschrift. 1952; 26: 112-137.
920 24. Pflug HD. Palyno-Stratigraphie des Eozän/Oligozän im Raum von Helmstedt, in
921 Nordhessen und im südlichen Anschlussbereich. In: Tobien H, editor. Nordwestdeutschland im
922 Tertiär. Beiträge zur Regionalen Geologie der Erde, Gebrüder Borntraeger, Berlin, Stuttgart.
923 1986; 18: pp. 567-582.
924 25. Laskar J, Fienga A, Gastineau M, Manche H. La2010. A new orbital solution for the long
925 term motion of the Earth. Astronomy & Astrophysics. 2011; 532, A89: 1-15.
926 26. Haq BU, Hardenbol J, Vail PR. Mesozoic and Cenozoic chronostratigraphy and cycles of
927 sea-level change. In: Wilgus CK, Hastings BS, Kendall, CGSG, Posamentier HW, Ross CA,
928 Van Wagoner JC, editors. Sea-level changes: an integrated approach. SEPM Special Publication.
929 1988; 42: pp. 71-108.
930 27. Riegel W, Wilde V. An early Eocene Sphagnum bog at Schöningen, northern Germany.
931 International Journal of Coal Geology. 2016; 159: 57-70.
932 28. Bujak JP, Brinkhuis H. Global warming and dinocyst changes across the Paleocene/Eocene
933 Epoch boundary. In: Aubry MP, Lucas SG, Berggren W, editors. Late Paleocene – early Eocene
934 climatic and biotic events in the marine and terrestrial records; 1998. pp. 277-295.
935 29. Crouch EM, Heilmann-Clausen C, Brinkhuis H, Morgans HE, Rogers KM, Egger H,
936 Schmitz B. Global dinoflagellate event associated with the late Paleocene thermal maximum.
937 Geology. 2001; 29: 315-318.

938 30. Heilmann-Clausen C, Nielsen OB, Gersner F. Lithostratigraphy and depositional
939 environments in the Upper Paleocene and Eocene of Denmark, Bulletin of the Geological
940 Society of Denmark. 1985; 33: 287-323.
941 31. Iakovleva AI, Brinkhuis H, Cavagnetto C. Late Palaeocene–Early Eocene dinoflagellate
942 cysts from the Turgay Strait, Kazakhstan; correlations across ancient seaways, Palaeogeography,
943 Palaeoclimatology, Palaeoecology. 2001; 172: 243-268.
944 32. Sluijs A, Brinkhuis, H. A dynamic climate and ecosystem state during the Paleocene-
945 Eocene Thermal Maximum: inferences from dinoflagellate cyst assemblages on the New Jersey
946 Shelf. Biogeosciences. 2009; 6: 1755-1781.
947 33. Sluijs A, Schouten S, Pagani M, Woltering M, Brinkhuis H, Damsté JSS, et al. Subtropical
948 Arctic Ocean temperatures during the Palaeocene/Eocene thermal maximum. Nature. 2006; 441:
949 610-613.
950 34. Sluijs A, Brinkhuis H, Schouten S, Bohaty SM, John CM, Zachos JC, et al. Environmental
951 precursors to rapid light carbon injection at the Palaeocene/Eocene boundary. Nature. 2007; 450:
952 1218-1221.
953 35. Williams GL, Damassa SP, Fensome RA, Guerstein GR. Wetzeliella and Its Allies — The
954 'Hole' Story: A Taxonomic Revision of the Paleogene Dinoflagellate Subfamily
955 Wetzelielloideae. Palynology. 2015; 39: 289-344.
956 36. Heilmann-Clausen C. Observations of the dinoflagellate Wetzeliella in Sparnacian facies
957 (Eocene) near Epernay, France, and a note on tricky acmes of Apectodinium. Proceedings of
958 the Geologists' Association. 2018. https://doi.org/10.1016/j.pgeola.2018.06.001
959 37. Kaiser ML, Ashraf R. Gewinnung und Präparation fossiler Pollen und Sporen sowie anderer
960 Palynomorphae unter besonderer Berücksichtigung der Siebmethode. Geologisches Jahrbuch.
961 1974; 25, 85–114.

962 38. Thomson PW, Pflug H. Pollen und Sporen des mitteleuropäischen Tertiärs.
963 Gesamtübersicht über die stratigraphisch und paläontologisch wichtigen Formen.
964 Palaeontographica B. 1953; 94: 1–138.
965 39. Krutzsch W, Vanhoorne R. Die Pollenflora von Epinois und Loksbergen in Belgien.
966 Palaeontographica B. 1977; 163: 1-110.
967 40. Thiele-Pfeiffer H. Die Mikroflora aus dem mitteleozänen Ölschiefer von Messel bei
968 Darmstadt. Palaeontographica B. 1988; 211: 1–86.
969 41. Nickel B. Die mitteleozäne Mikroflora von Eckfeld bei Manderscheid/Eifel. Mainzer
970 Naturwissenschaftliches Archiv. Beiheft. 1996; 18: 1–121.
971 42. Lenz OK, Wilde V. Changes in Eocene plant diversity and composition of vegetation: the
972 lacustrine archive of Messel (Germany). Paleobiology. 2018; 44: 709-735.
973 43. Moshayedi M, Lenz OK, Wilde V, Hinderer M. The recolonization of volcanically
974 disturbed Eocene habitats of Central Europe: The maar lakes of Messel and Offenthal (SW
975 Germany) compared. Palaeobiodiversity and Palaeoenvironments. 2020 (in press)
976 44. Bray JR, Curtis JT. An ordination of the upland forest communities of southern Wisconsin.
977 Ecological Monographs. 1957; 27: 325-349.
978 45. Cottam G, Goff FG, Whittaker RH. Wisconsin Comparative Ordination. In: Whittaker RH,
979 editor. Ordination of Plant Communities. Handbook of Vegetation Science. 1978; 5-2: 185-213.
980 46. Gauch HG, Scruggs WM. Variants of polar ordination. Vegetatio. 1979; 40: 147-153.
981 47. Oksanen J. Standardization methods for community ecology. Documentation and user
982 guide for package Vegan, 1.8-6; 2007.
983 48. Mander L, Kürschner WM, McElwain JC. An explanation for conflicting records of
984 Triassic–Jurassic plant diversity. Proceedings of the National Academy of Sciences of the
985 United States of America. 2010; 107: 15351–15356.

986 49. Hammer Ø, Harper DAT, Ryan PD. PAST: paleontological statistics software package for
987 education and data analysis. Palaeontologia Electronica. 2001; 4. Available from:
988 http://www.palaeo-electronica.org/2001_1/past/issue1_01.htm.
989 50. Hair JF, Black WC, Babin BJ, Anderson RE. Multivariate Data Analysis. Seventh Edition.
990 Prentice Hall, Upper Saddle River, New Jersey; 2010.
991 51. Minchin PR. An evaluation of the relative robustness of techniques for ecological
992 ordination. Vegetatio. 1987; 69: 89–107.
993 52. Jardine PE, Harrington GJ. The Red Hills Mine palynoflora: A diverse swamp assemblage
994 from the Late Paleocene of Mississippi, USA. Palynology. 2008; 32: 183-204.
995 53. Ghilardi B, O'Connell M. Fine resolution pollen analytical study of Holocene woodland
996 dynamics and land use in north Sligo, Ireland. Boreas. 2013; 42: 623-649.
997 54. Broothaerts N, Verstraeten G, Kasse C, Bohncke S, Notebaert B, Vandenberghe J.
998 Reconstruction and semi-quantification of human impact in the Dijle catchment, central
999 Belgium: a palynological and statistical approach. Quaternary Science Reviews. 2014; 102: 96-
1000 110.
1001 55. Borsch T, Wilde V. Pollen variability within species, populations, and individuals, with
1002 particular reference to *Nelumbo nucifera*. In: Harley M, Blackmore S, Morton C, editors. Pollen
1003 and Spores: Morphology and Biology. Royal Botanic Gardens, Kew; 2000. pp. 285-299.
1004 56. Colwell RK, Chao A, Gotelli NJ, Lin SY, Mao CX, Chazdon RL, Longino JT. Models and
1005 estimators linking individual-based and sample-based rarefaction, extrapolation, and
1006 comparison of assemblages. Journal of Plant Ecology. 2012; 5, 3-21.
1007 57. Colwell RK. EstimatesS: Statistical estimation of species richness and shared species from
1008 samples. Version 9. 2013. Available from: http://viceroy.eeb.uconn.edu/EstimateS/

1009 58. Keen HF, Gosling WD, Hanke F, Miller CS, Montoya E, Valencia BG, Williams JJ. A
1010 statistical sub-sampling tool for extracting vegetation community and diversity information
1011 from pollen assemblage data. Palaeogeography, Palaeoclimatology, Palaeoecology. 2014; 408:
1012 48-59.
1013 59. Whittaker RH. Evolution and measurement of species diversity. Taxon. 1972; 21: 213-251.
1014 60. Harrington GJ, Jaramillo CA. Paratropical floral extinction in the Late Palaeocene–Early
1015 Eocene. Journal of the Geological Society London. 2007; 164: 323–332.
1016 61. Birks HJB, Felde VA, Bjune AE, Grytnes JA, Seppä H, Giesecke T. Does pollen-
1017 assemblage richness reflect floristic richness? A review of recent developments and future
1018 challenges. Review of Palaeobotany and Palynology. 2016; 228: 1–25.
1019 62. Ellison AM. Partitioning diversity. Ecology. 2010; 91: 1962–1963.
1020 63. Beck J, Holloway JD, Schwanghart W. Undersampling and the measurement of beta
1021 diversity. Methods in Ecology and Evolution. 2013; 4: 370–382.
1022 64. Whittaker RH. Vegetation of the Siskiyou mountains, Oregon and California. Ecological
1023 Monographs. 1960; 30: 279–338.
1024 65. Koleff P, Gaston KJ, Lennon JJ. Measuring beta diversity for presence–absence data.
1025 Journal of Animal Ecology. 2003; 72: 367–382.
1026 66. Gotelli NJ, Colwell, RK. Estimating species richness. In Magurran AE, McGill BJ, editors.
1027 Biological diversity. Frontiers in measurement and assessment. Oxford University Press, New
1028 York; 2010. pp. 39-54.
1029 67. Smith B, Wilson JB. A consumer's guide to evenness indices. Oikos. 1996; 76: 70–82.
1030 68. Inglis GN, Collinson ME, Riegel W, Wilde V, Robson BE, Lenz OK, Pancost RD.
1031 Ecological and biogeochemical change in an early Paleogene peat-forming environment:

Linking biomarkers and palynology, Palaeogeography, Palaeoclimatology, Palaeoecology. 2015; 438: 245-255.

69. Gastaldo RA, Allen GP, Huc AY. Detrital peat formation in the tropical Mahakam River delta, Kalimantan, eastern Borneo: Sedimentation, plant composition, and geochemistry. In: Cobb JC, Blaine C, editors. Modern and Ancient Coal-Forming Environments Mires: Geological Society of America Special Paper. 1993; 286: pp. 107–118.

70. Gastaldo, RA. The genesis and sedimentation of phytoclasts with examples from coastal environments. In: Traverse A, editor. Sedimentation of Organic Particles. Cambridge University Press; 1994. pp. 103-127.

71. Krebs CJ. Ecological methodology. Harper and Row Publishers Inc., New York, NY; 1989.

72. Smith AHV. The sequence of microspore assemblages associated with the occurrence of crassidurite in coal seams of Yorkshire. Geological Magazine. 1957; 94: 345-363.

73. Smith AHV. The palaeoecology of carboniferous peats based on the miospores and petrography of bitmminous coals. Proceedings of the Yorkshire Geological Society. 1962; 33: 423-474.

74. Smith AVH. Seam profiles and seam characters. In: Murchison D, Westoll TS, editors. Coal and coal-bearing strata. Elsevier, New York.;1968. pp. 31-40.

75. Dai S, Bechtel A, Eble CF, Flores RM, French D, Graham IT, et al. Recognition of peat depositional environments in coal: A review. International Journal of Coal Geology. 2020. doi: 10.1016/j.coal.2019.103383

76. Teichmüller M. Rekonstruktion verschiedener Moortypen des Hauptflözes der niederrheinischen Braunkohle. Fortschritte der Geologie des Rheinlandes und Westfalen.1958; 2: 539-612.

1055 77. Teichmüller M. The genesis of coal from the viewpoint of coal petrology. International
1056 Journal of Coal Geology. 1989; 12: 1-87.
1057 78. Lenz OK, Riegel W. Isopollen maps as a tool for the reconstruction of a coastalswamp from
1058 the Middle Eocene at Helmstedt (Northern Germany). Facies. 2001; 45: 177–194.
1059 79. Wilde V, Lenz OK, Riegel W. Mangrove structure and development in the Lower and
1060 Middle Eocene of Helmstedt, northern Germany. Terra Nostra. 2008; 2: 306-307.
1061 80. Natlandsmyr B, Hjelle KL. Long-term vegetation dynamics and land-use history: Providing
1062 a baseline for conservation strategies in protected *Alnus glutinosa* swamp woodlands. Forest
1063 Ecology and Management. 2016; 372: 78-92.
1064 81. Houston DT, de Rigo D, Caudullo G. *Alnus incana* in Europe: distribution, habitat, usage
1065 and threats. In: San-Miguel-Ayanz J, de Rigo D, Caudullo G, Houston DT, Mauri A. editors.
1066 European Atlas of Forest Tree Species. Luxembourg: Publication Office of the European Union;
1067 2016. pp. e01ff87+.
1068 82. Fralish JS, Franklin SB. Taxonomy and Ecology of Woody Plants in North American
1069 Forests (Excluding Mexico and Subtropical Florida). New York: John Wiley & Sons; 2002.
1070 83. Davis JH. The peat deposits of Florida; their occurrence, development and uses. Florida
1071 Geological Survey Bulletin. 1946; 30: 1-247.
1072 84. Spackman W, Riegel WL, Dolsen CP. Geological and biological interactions in the swamp-
1073 marsh complex of Southern Florida. In: Dapples EC, Hopkins ME, editors. Environments of
1074 Coal Deposition. Geological Society of America, Special Paper. 1969; 114: pp. 1-35.
1075 85. Moore PD. Ecological and hydrological aspects of peat formation. In: Scott AC, editor.
1076 Coal and Coal-bearing Strata: Recent Advances. Geological Society, London, Special
1077 Publications. 1987; 32: pp. 7-16.

1078 86. Moore TA, Hilbert RE. Petrographic and anatomical characteristics of plant material from
1079 two peat deposits of Holocenc and Miocene age, Kalimantan, Indonesia. Review of
1080 Palaeobotany and Palynology. 1992; 72: 199-227.
1081 87. Simpson MJA., Macintosh DF, Cloughley JB., Stuart AE. Past, present and future
1082 utilisation of *Myrica gale* (Myricaceae). Economic Botany. 1996; 50: 122-129.
1083 88. Skene KR, Sprent JI, Raven JA, Herdman L. Myrica gale L. Biological flora of the British
1084 Isles. Journal of Ecology 2000; 88: 1079–1094.
1085 89. van Breemen N. How Sphagnum bogs down other plants. Trends in Ecology & Evolution.
1086 1995; 10: 270–275.
1087 90. Clymo R. 1984. The limits to peat bog growth. Philosophical Transactions of the Royal
1088 Society B. 1984; B 303 (1117): 605–654.
1089 91. Page SE, Rieley JO, Shotyk W, Weiss D. Interdependence of peat and vegetation in tropical
1090 swamp forest. Philosophical Transactions of the Royal Society B. 1999; 354: 1885-1897.
1091 92. Hochuli PA. Ursprung und Verbreitung der Restionaceen. Vierteljahrsschrift der
1092 Naturforschenden Gesellschaft Zürich. 1979; 124: 109–130.
1093 93. Heywood VH. Flowering Plants of the World. Updated ed. Oxford University Press, New
1094 York; 1993.
1095 94. Daly RJ, Jolley DW. What was the nature and role of Normapolles angiosperms? A case
1096 study from the earliest Cenozoic of Eastern Europe. Palaeogeography, Palaeoclimatology,
1097 Palaeoecology. 2015; 418: 141-149.
1098 95. Loftin SS, Guyette MQ, Wetzel PR. Evaluation of Vegetation-Fire Dynamics in the
1099 Okefenokee National Wildlife Refuge, Georgia, USA, with Bayesian Belief Networks.
1100 Wetlands. 2018; 38: 819-834.

1101 96. Cypert E. The effect of fires in the Okefenokee Swamp in 1954 and 1955. The American
1102 Midland Naturalist. 1961; 66: 485-503.
1103 97. Cohen AD. Petrography and paleoecology of Holocene peats from the Okefenokee swamp-
1104 marsh complex of Georgia. Journal of Sedimentary Petrology.1974; 44: 716-726.
1105 98. Izlar, RL. Some comments on fire and climate in the Okefenokee swamp-marsh complex.
1106 In: Cohen AD, Casagrande DJ, Andrejko MJ, Best GR, editors. The Okefenokee swamp: its
1107 natural history, geology and geochemistry. 1984. pp. 70-85.
1108 99. Harrington GJ. Impact of Paleocene/Eocene Greenhouse Warming on North American
1109 Paratropical Forests. Palaios. 2001; 16: 266–278.
1110 100. Harrington GJ. Geographic patterns in the floral response to Paleocene–Eocene warming.
1111 In: Wing SL, Gingerich PD, Schmitz B, Thomas E, editors. Causes and consequences of
1112 globally warm climates in the early Paleogene. Geological Society of America, Special Paper.
1113 2003; 369: pp. 381–393.
1114 101. Page SE, Rieley JO, Wust R. Chapter 7. Lowland tropical peatlands of Southeast Asia. In:
1115 Martini IP, Martinez Cortizas A., Chesworth W, editors. Developments in Earth Surface
1116 Processes. Peatlands — Evolution and Records of Environmental and Climate Changes. 2006;
1117 9: pp. 145–172.
1118 102. Phillips S, Rouse GE, Bustin RM. Vegetation zones and diagnostic pollen profiles of a
1119 coastal peat swamp, Bocas del Toro, Panamá. Palaeogeography, Palaeoclimatology,
1120 Palaeoecology. 2001; 128: 301-338.
1121 103. Inglis GN, Collinson ME, Riegel W, Wilde V, Farnsworth A, Lunt DJ, et al. Mid-latitude
1122 continental temperatures through the early Eocene in western Europe. Earth and Planetary
1123 Science Letters. 2017; 460: 86-96.

104. Collinson ME, Steart DC, Harrington GJ, Hooker JJ, Scott AC, Allen LO, Glasspool IJ, Gibbonsm SJ. Palynological evidence of vegetation dynamics in response to palaeoenvironmental change across the onset of the Paleocene-Eocene Thermal Maximum at Cobham, Southern England. Grana. 2009; 48: 38-66.

105. Garel S, Schnyder J, Jacob J, Dupuis C, Boussafir M, Le Milbeau C, Storme JY, Iakovleva AI, Yans J, Baudin F. Paleohydrological and paleoenvironmental changes recorded in terrestrial sediments of the Paleocene–Eocene boundary (Normandy, France). Palaeogeography, Palaeoclimatology, Palaeoecology. 2013; 376: 184–199.

106. Greenwood DR, Basinger JF. The paleoecology of high-latitude Eocene swamp forests from Axel Heiberg Island, Canadian High Arctic. Review of Palaeobotany and Palynology. 2013; 81: 83-97.

107. Eldrett JS, Greenwood DR, Polling M, Brinkhuis H, Sluijs A. A seasonality trigger for carbon injection at the Paleocene–Eocene Thermal Maximum. Climate of the Past. 2014; 10: 759–769.

108. Weijers JWH, Schouten S, Sluijs A, Brinkhuis H, Sinninghe Damsté JS. Warm arctic continents during the Palaeocene–Eocene thermal maximum. Earth and Planetary Science Letters. 2007; 261: 230–238.

109. Nichols DJ, Pocknall DT. Relationships of palynofacies to coal-depositional environments in the upper Paleocene of the Gulf Coast Basin, Texas, and the Powder River Basin, Montana and Wyoming. Traverse A, editor. Sedimentation of Organic Particles. Cambridge University Press, Cambridge; 1994. pp. 217-237.

110. Collinson ME, Hooker JJ, Gröcke DR. Cobham Lignite Bed and penecontemporaneous macrofloras of southern England: A record of vegetation and fire across the Paleocene-Eocene Thermal Maximum. Geological Society of America, Special Paper. 2003; 369: 333 – 349.

111. Kurtz AC, Kump LR, Arthur MA, Zachos JC, Paytan A. Early Cenozoic decoupling of the global carbon and sulphur cycles. Palaeoceanography. 2003; 18: 1090–1104.

112. Moore EA, Kurtz AC. Black carbon in Paleocene–Eocene boundary sediments: A test of biomass combustion as the PETM trigger. Palaeogeography, Palaeoclimatology, Palaeoecology. 2008; 267: 147–152.

Supporting information

S1 Appendix. Taxonomic list.

Complete list of palynomorphs from the studied sections N, S1, S2 from Seam 1 of the Schöningen Formation including their systematic affinities. In the left column the 45 "variables" are presented, which were used for the pollen diagrams and statistical analysis (cluster analysis, non-metric multidimensional scaling).

S1 Table: Raw data set of section N.

The data have been used for pollen diagram, cluster analysis and NMDS.

S2 Table: Raw data set of section S1 (a).

The data have been used for pollen diagram, cluster analysis and NMDS.

S3 Table: Raw data set of section S2

The data have been used for pollen diagram, cluster analysis and NMDS.

S4 Table: Raw data set of section S1 (b)

1171 The data have been used for diversity analysis.

1172

1173 **S5 Table: Estimations of beta diversity for Seam 1 in section S1.**

1174 Given are pairwise comparisons of 11 lignite samples from section S1 using the measure of [59,

1175 64]: (S/ā) – 1; S, total number of species in the two compared samples, ā, average number of species

1176 in the two compared samples of Seam 1.

1177

1178

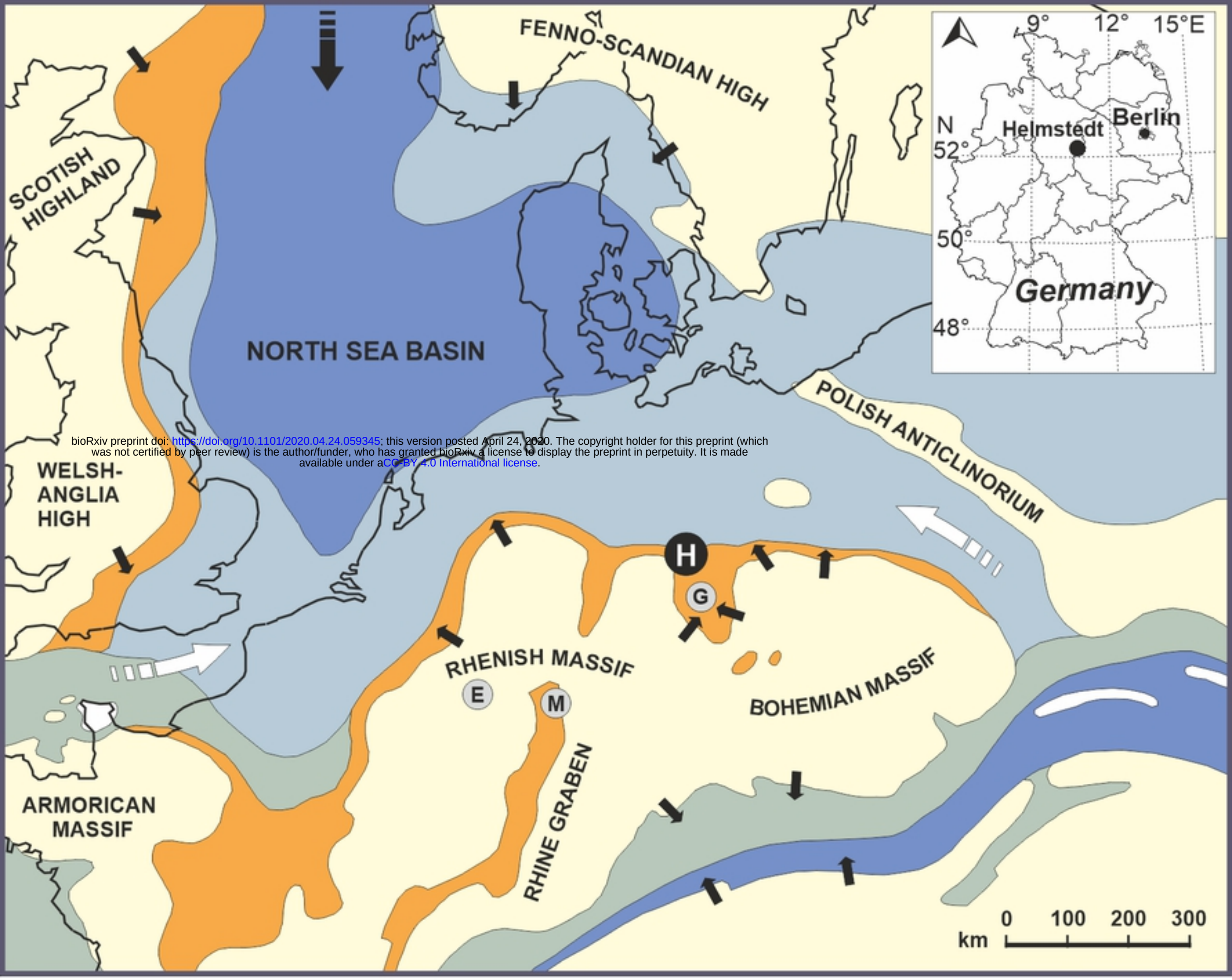

No sedimentation

Terrestrial facies

Marine-terrestrial clastic facies

Marine facies with shallow water carbonates

Marine facies with clays

direction of sediment input

Tethyal current

Boreal current

H Helmstedt/Schöningen

Other Middle Eocene fossil localities:

G Geiseltal M Messel E Eckfeld

Figure 01

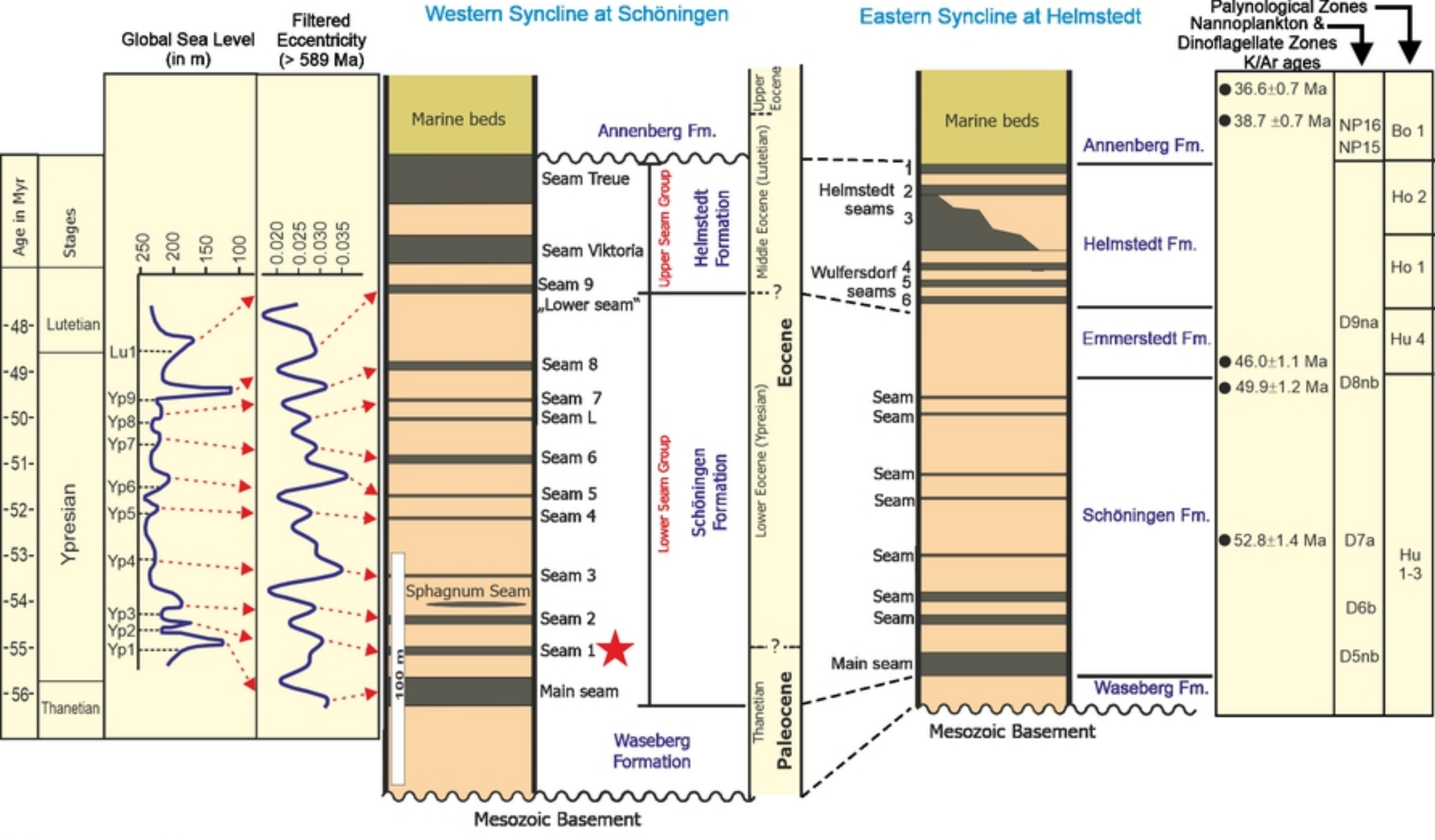
Western Syncline at Schöningen
Eastern Syncline at Helmstedt
Global Sea Level (in m)
Filtered Eccentricity (> 589 Ma)
Palynological Zones
Nannoplankton & Dinoflagellate Zones
K/Ar ages
Age in Myr
Stages
Lutetian
Ypresian
Thanetian
Lu1
Yp9
Yp8
Yp7
Yp6
Yp5
Yp4
Yp3
Yp2
Yp1
Marine beds
Annenberg Fm.
Seam Treue
Seam Viktoria
Seam 9
„Lower seam"
Seam 8
Seam 7
Seam L
Seam 6
Seam 5
Seam 4
Seam 3
Sphagnum Seam
Seam 2
Seam 1
Main seam
100 m
Upper Seam Group
Helmstedt Formation
Lower Seam Group
Schöningen Formation
Waseberg Formation
Mesozoic Basement
Upper Eocene
Middle Eocene (Lutetian)
Lower Eocene (Ypresian)
Eocene
Paleocene
Helmstedt seams
Wulfersdorf seams
Emmerstedt Fm.
Helmstedt Fm.
Schöningen Fm.
Waseberg Fm.
36.6±0.7 Ma
38.7 ±0.7 Ma
46.0±1.1 Ma
49.9±1.2 Ma
52.8±1.4 Ma
NP16
NP15
D9na
D8nb
D7a
D6b
D5nb
Bo 1
Ho 2
Ho 1
Hu 4
Hu 1-3

Figure 02

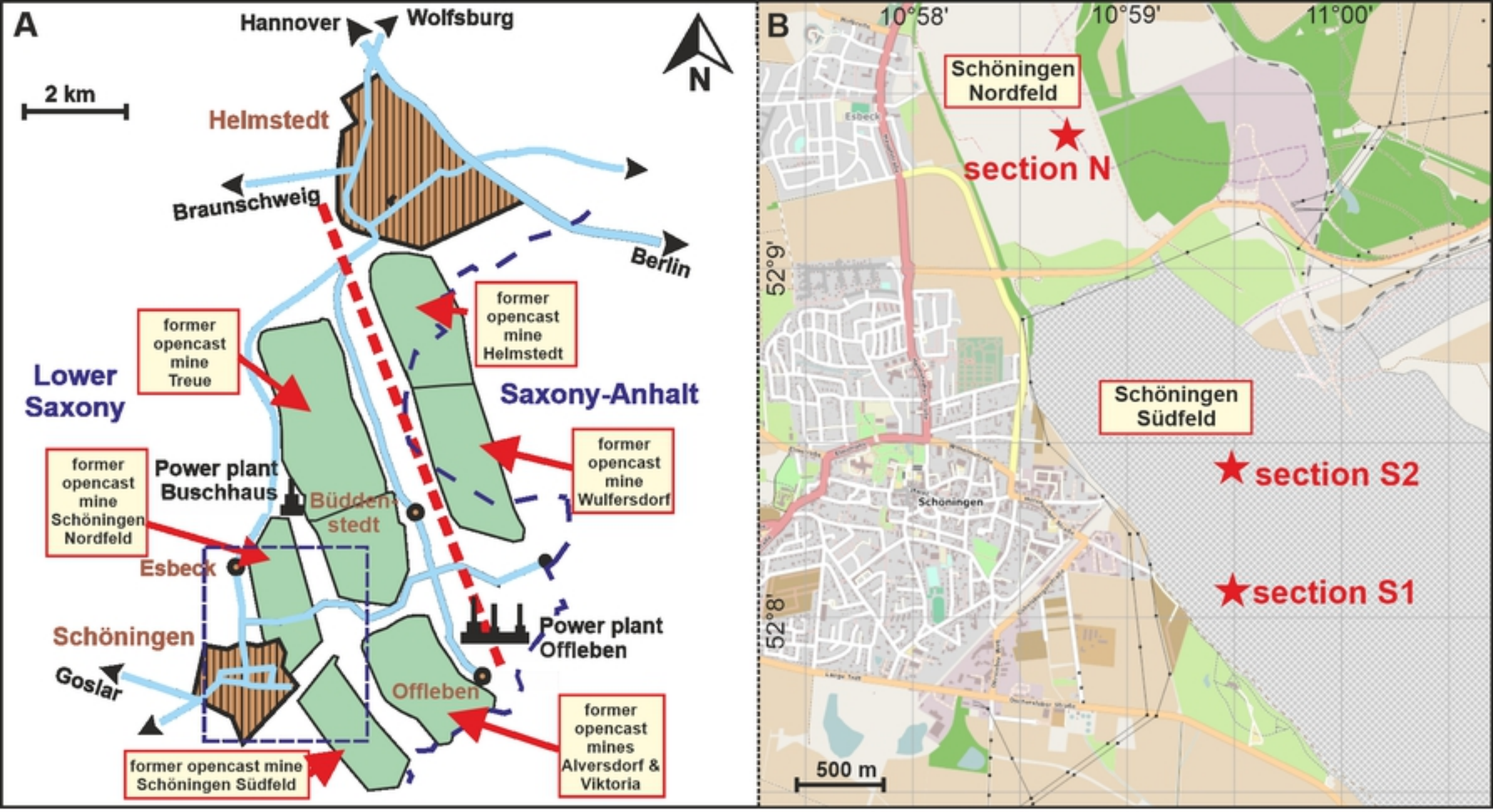
A
Hannover
Wolfsburg
N
2 km
Helmstedt
Braunschweig
Berlin
former opencast mine Helmstedt
former opencast mine Treue
Lower Saxony
Saxony-Anhalt
former opencast mine Schöningen Nordfeld
Power plant Buschhaus
Büddenstedt
former opencast mine Wulfersdorf
Esbeck
Schöningen
Power plant Offleben
Goslar
Offleben
former opencast mine Schöningen Südfeld
former opencast mines Alversdorf & Viktoria
B
10°58'
10°59'
11°00'
Schöningen Nordfeld
section N
52°9'
52°8'
Schöningen Südfeld
section S2
section S1
500 m

Figure 03

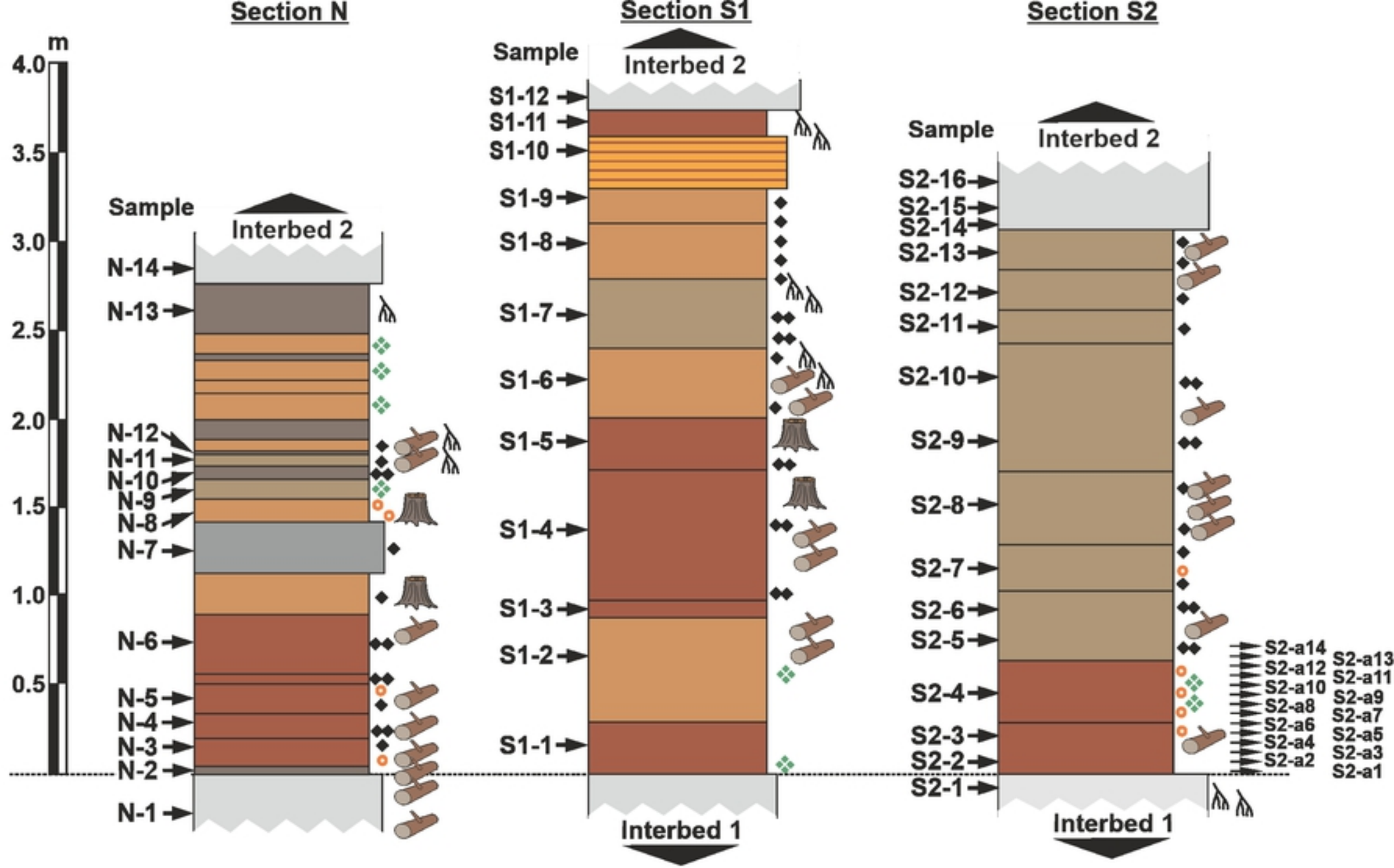
Section N
Section S1
Section S2
m
4.0
3.5
3.0
2.5
2.0
1.5
1.0
0.5
Sample
Interbed 2
N-14
N-13
N-12
N-11
N-10
N-9
N-8
N-7
N-6
N-5
N-4
N-3
N-2
N-1
S1-12
S1-11
S1-10
S1-9
S1-8
S1-7
S1-6
S1-5
S1-4
S1-3
S1-2
S1-1
S2-16
S2-15
S2-14
S2-13
S2-12
S2-11
S2-10
S2-9
S2-8
S2-7
S2-6
S2-5
S2-4
S2-3
S2-2
S2-1
S2-a14
S2-a13
S2-a12
S2-a11
S2-a10
S2-a9
S2-a8
S2-a7
S2-a6
S2-a5
S2-a4
S2-a3
S2-a2
S2-a1
Interbed 1
lignite: matrix dominated lithotype
lignite: tissue dominated lithotype
lignite: mixed tissue/matrix lithotype
clayey lignite
lignite: carbonaceous clay
lignite: mix of silt/sand and coal
interbed: silty clay to clayey silt
stump
xylite
root traces
fusite
resin
plant tissue

Figure 04

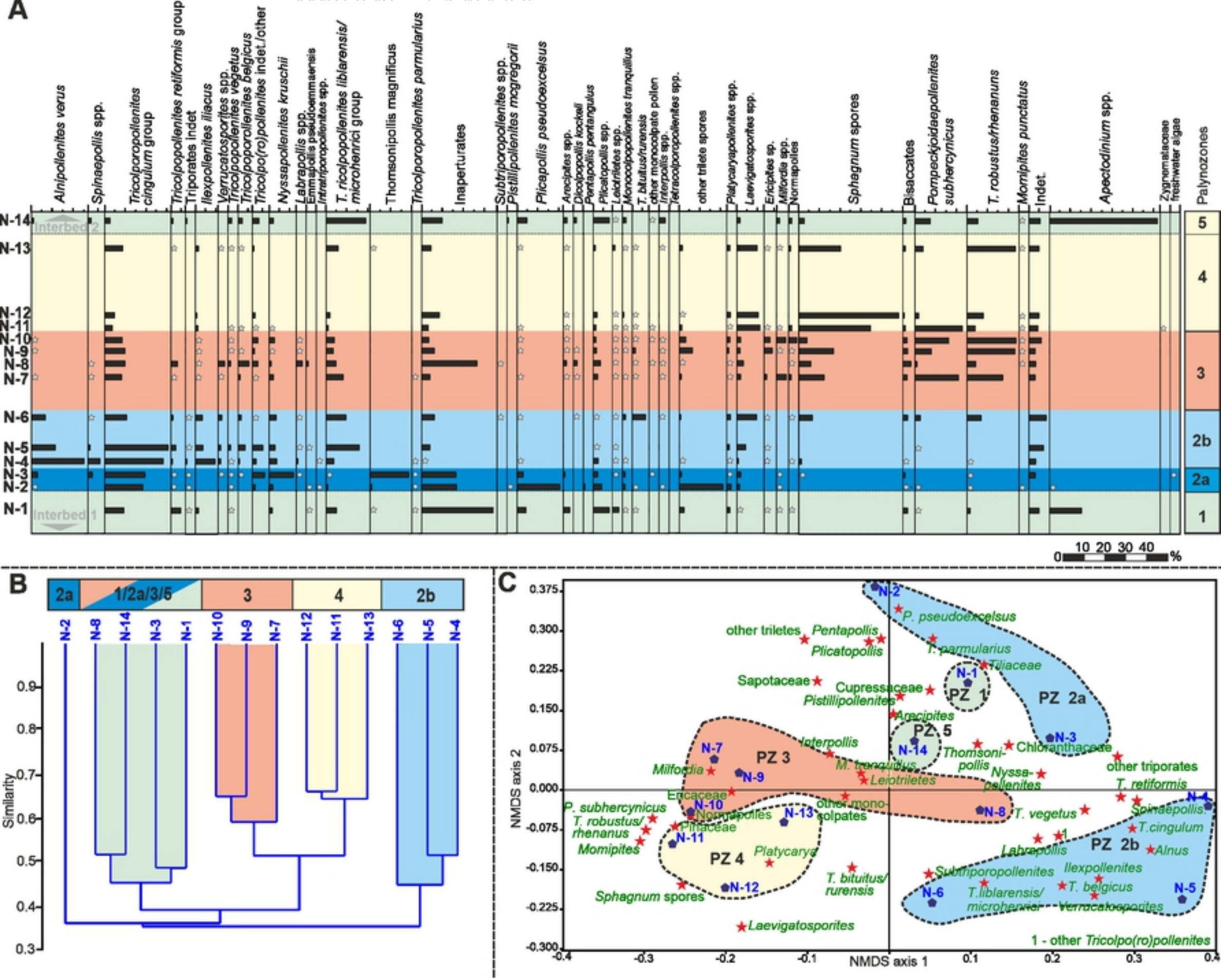
A
Alnipollenites verus
Spinaepollis spp.
Tricolporopollenites cingulum group
Tricolpopollenites retiformis group
Triporates indet
Ilexpollenites iliacus
Verrucatosporites spp.
Tricolpopollenites vegetus
Tricolpopollenites belgicus
Tricolpo(ro)pollenites indet./other
Nyssapollenites kruschii
Labrapollis spp.
Emmapollis pseudoemmaensis
intratriporopollenites spp.
T. ricolpopollenites liblarensis/ microhenrici group
Thomsonipollis magnificus
Tricolporopollenites parmularius
Inaperturates
Subtriporopollenites spp.
Pistillipollenites mcgregorii
Plicapollis pseudoexcelsus
Arecipites spp.
Dicolpopollis kockelii
Pentapollis pentangulus
Plicatopollis spp.
Leiotriletes spp.
Monocolpopollenites tranquillus
T. bituitus/rurensis
other monocolpate pollen
Interpollis spp.
Tetracolporopollenites spp.
other trilete spores
Platycaryapollenites spp.
Laevigatosporites spp.
Ericipites sp.
Milfordia spp.
Normapolles
Sphagnum spores
Bisaccates
Pompeckjoidaepollenites subhercynicus
T. robustus/rhenanus
Momipites punctatus
Indet.
Apectodinium spp.
Zygnemataceae freshwater algae
Palynozones
N-14
N-13
N-12
N-11
N-10
N-9
N-8
N-7
N-6
N-5
N-4
N-3
N-2
N-1
Interbed 2
Interbed 1
5
4
3
2b
2a
1
10 20 30 40
0
%
B
2a
1/2a/3/5
3
4
2b
N-2
N-8
N-14
N-3
N-1
N-10
N-9
N-7
N-12
N-11
N-13
N-6
N-5
N-4
Similarity
0.9
0.8
0.7
0.6
0.5
0.4
0.3
C
N-2
P. pseudoexcelsus
other trilete
Pentapollis
Pticatopollis
T. parmularius
Tiliaceae
N-1
PZ 1
PZ 2a
Sapotaceae
Cupressaceae
Pistillipollenites
Araciptes
PZ 5
N-14
N-3
Chloranthaceae
Interpollis
N-7
PZ 3
Thomsoni-pollis
other triporates
Milfordia
N-9
M. tranquillus
Leiotriletes
Nyssa-pollenites
T. retiformis
Ericaceae
P. subhercycnicus
N-10
other mono-colpates
N-8
T. vegetus
N-4
Spinaepollis
T. robustus/ rhenanus
Normapolles
N-13
T.cingulum
Pinaceae
N-11
PZ 2b
Labrapollis
Alnus
Momipites
PZ 4
Platycarya
Subtriporopollenites
Ilexpollenites
T. bituitus/ rurensis
T. belgicus
N-6
T.liblarensis/ microhenrici
Verrucatosporites
N-5
Sphagnum spores
N-12
Laevigatosporites
1 - other Tricolpo(ro)pollenites
NMDS axis 2
NMDS axis 1
0.375
0.300
0.225
0.150
0.075
0.000
-0.075
-0.150
-0.225
-0.300
-0.4
-0.3
-0.2
-0.1
0.1
0.2
0.3
0.4

Figure 05

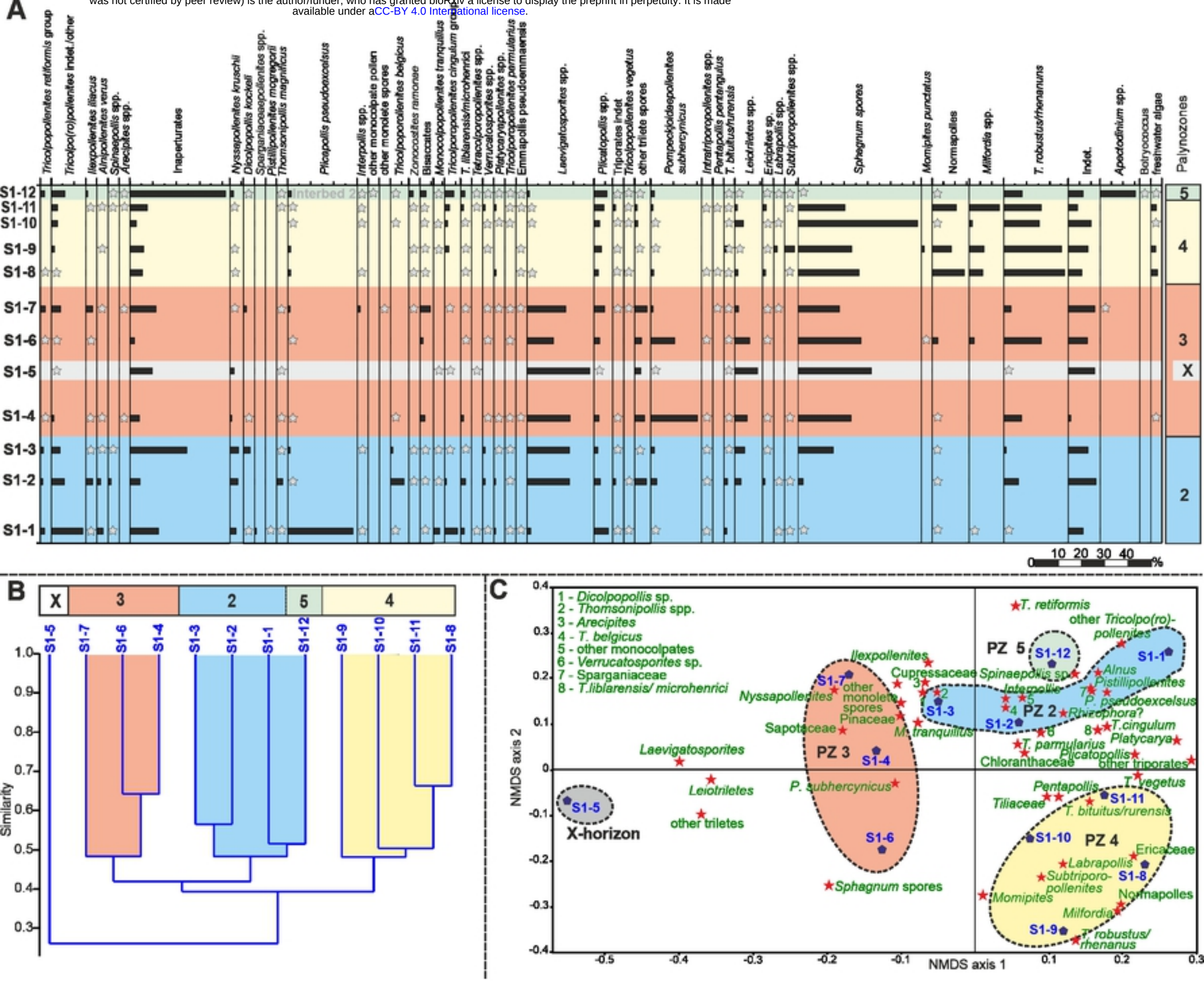

Figure 06

Figure 07

Figure 08

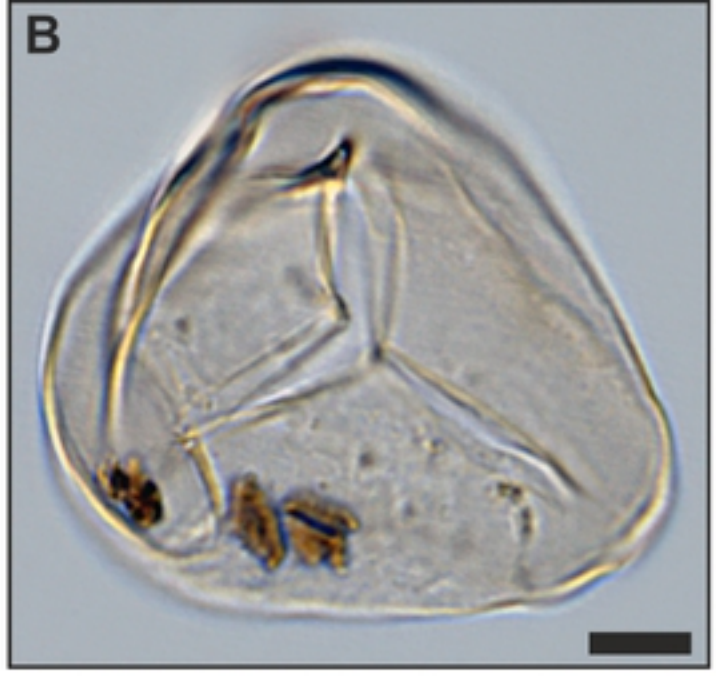

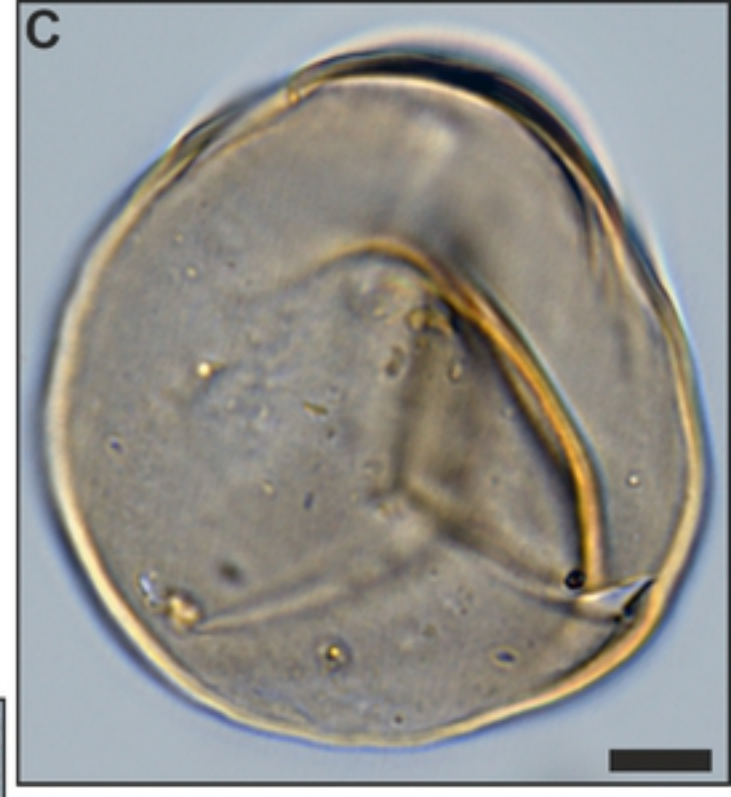

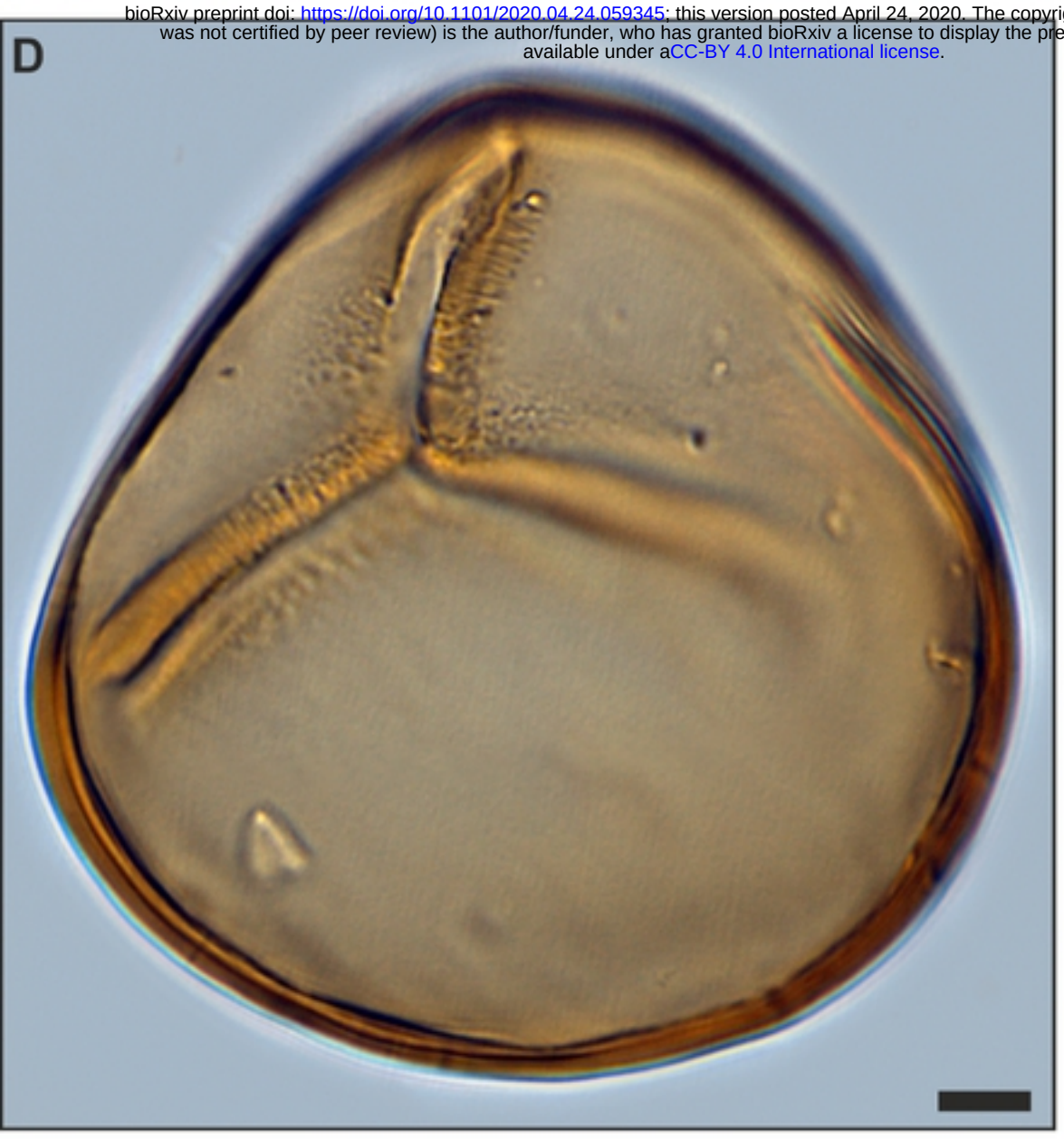

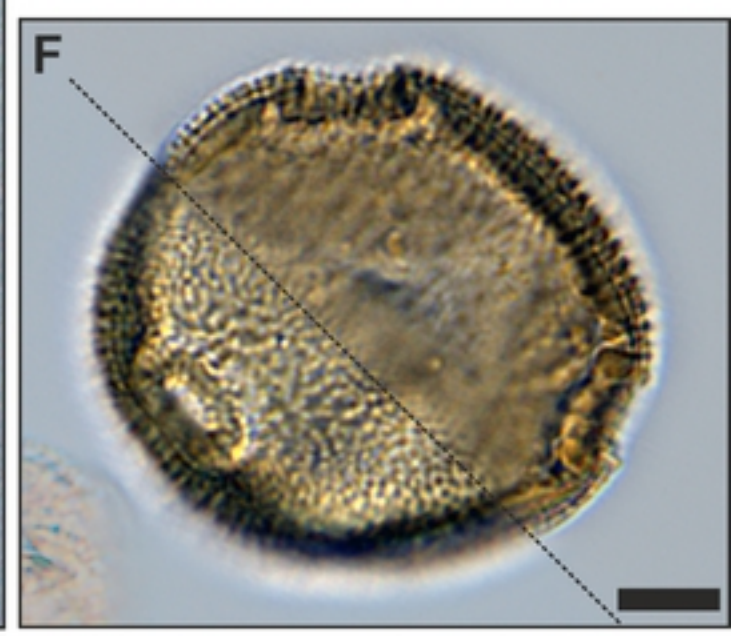

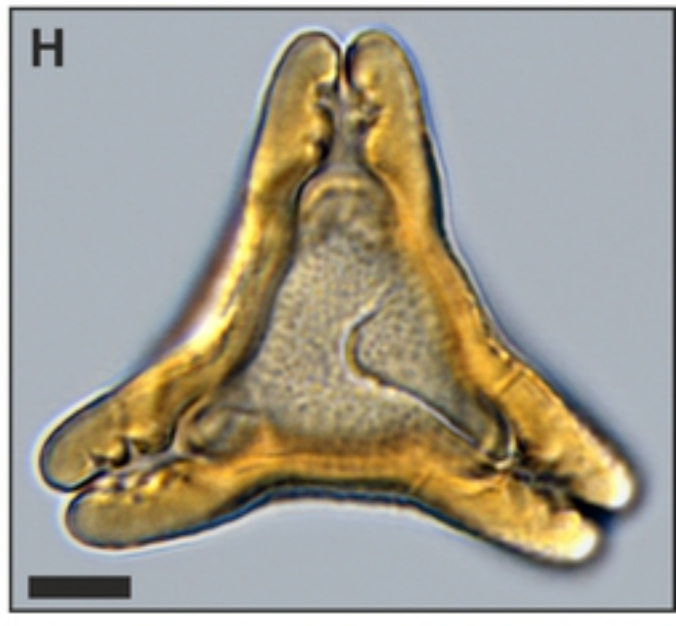

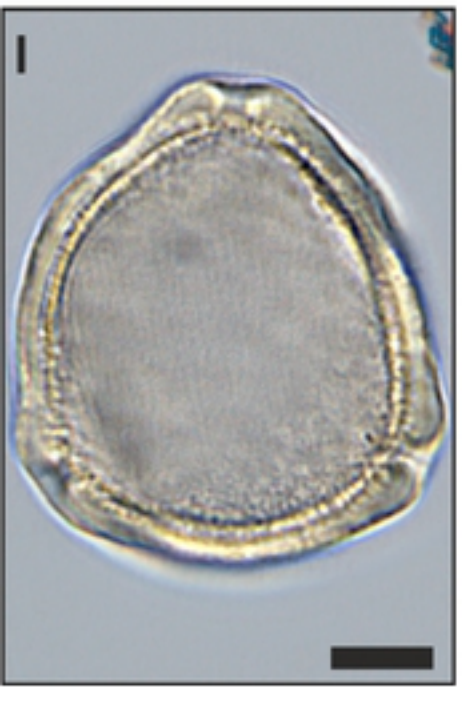

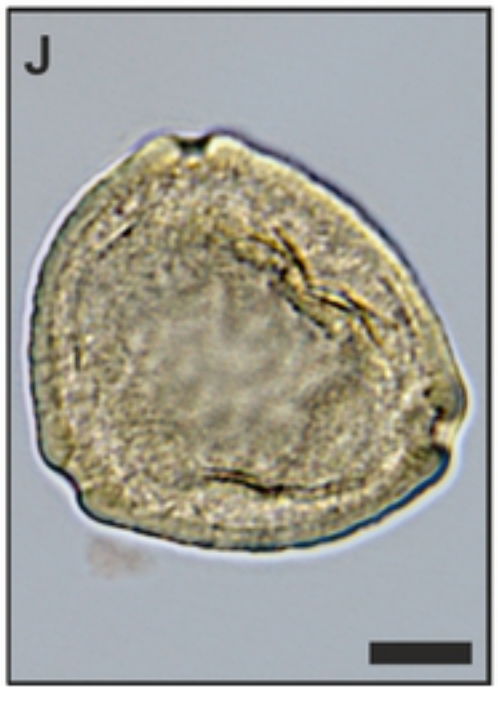

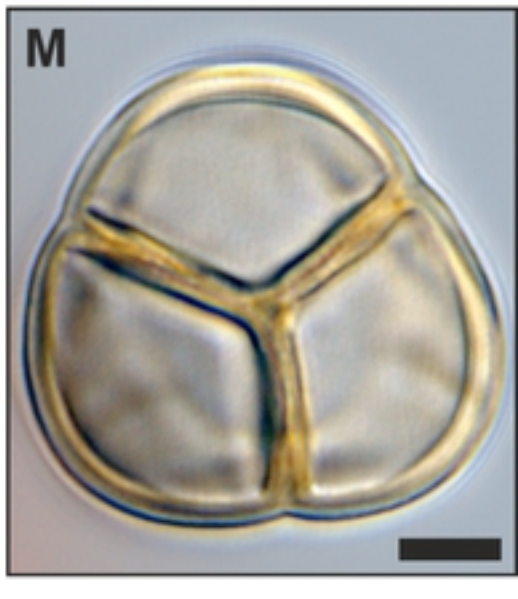

Figure 09

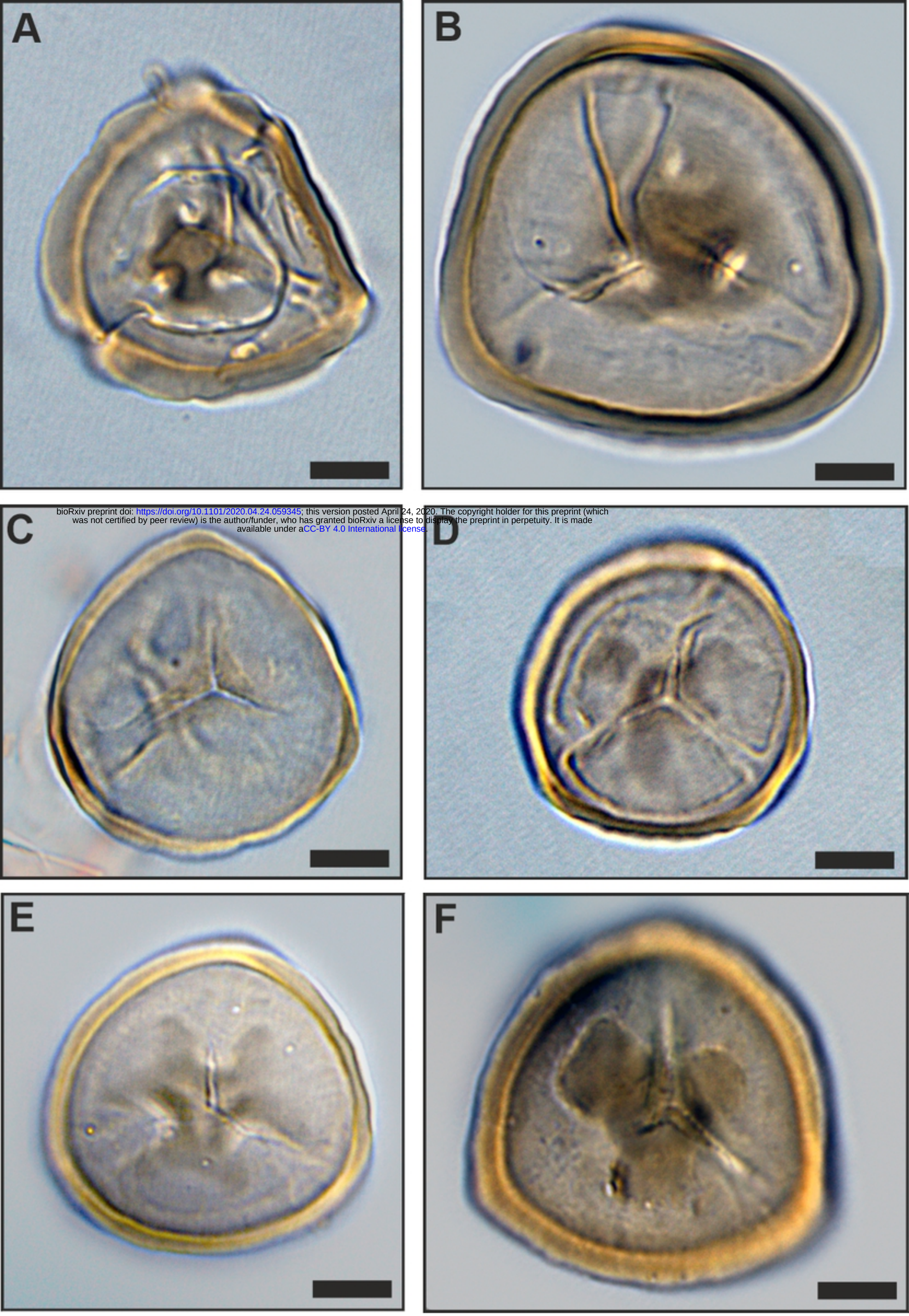

Figure 10

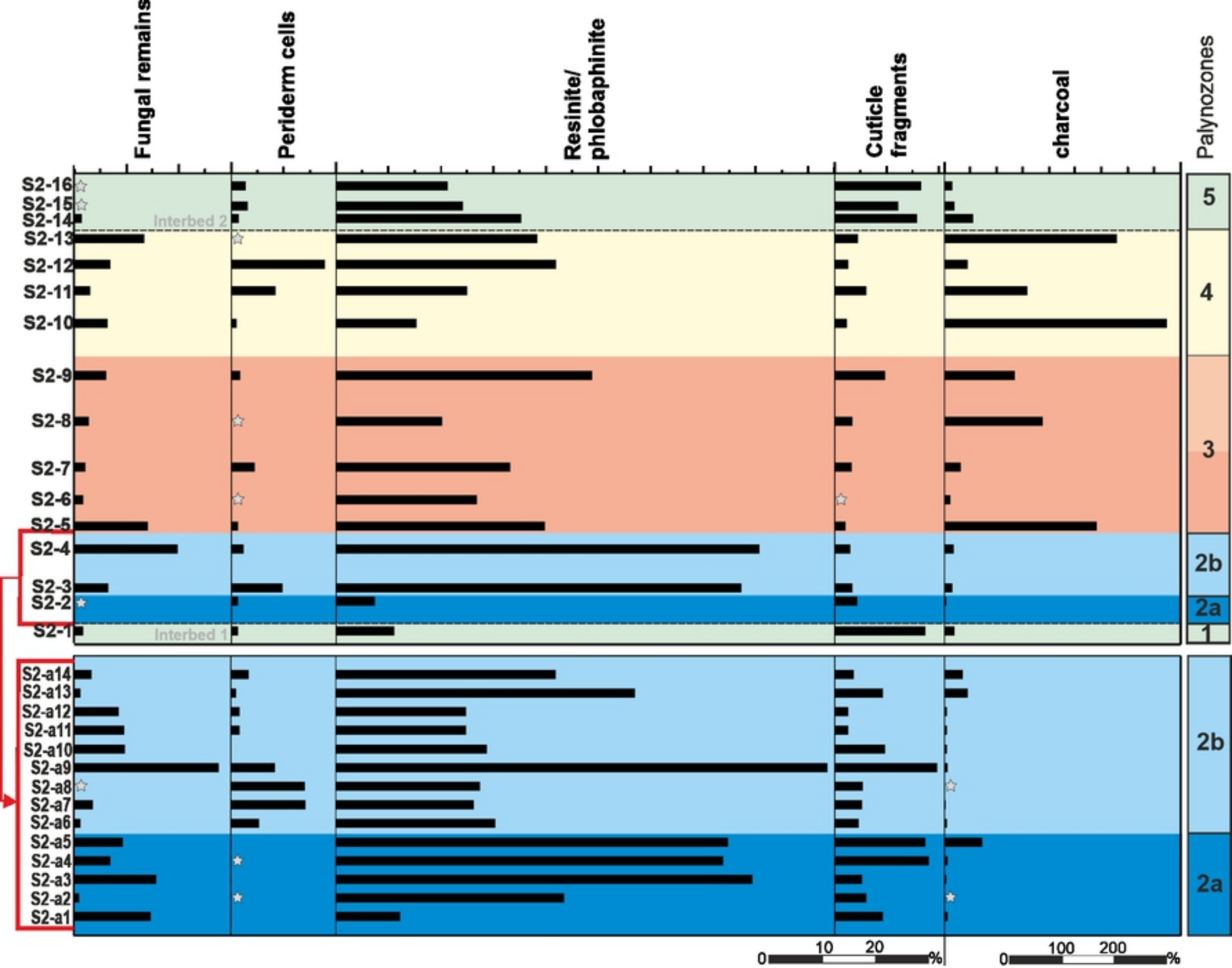
Fungal remains
Periderm cells
Resinite/ phlobaphinite
Cuticle fragments
charcoal
Palynozones
S2-16
S2-15
S2-14
Interbed 2
S2-13
S2-12
S2-11
S2-10
S2-9
S2-8
S2-7
S2-6
S2-5
S2-4
S2-3
S2-2
S2-1
Interbed 1
S2-a14
S2-a13
S2-a12
S2-a11
S2-a10
S2-a9
S2-a8
S2-a7
S2-a6
S2-a5
S2-a4
S2-a3
S2-a2
S2-a1
5
4
3
2b
2a
1
2b
2a
0
10
20
%
0
100
200
%

Figure 11

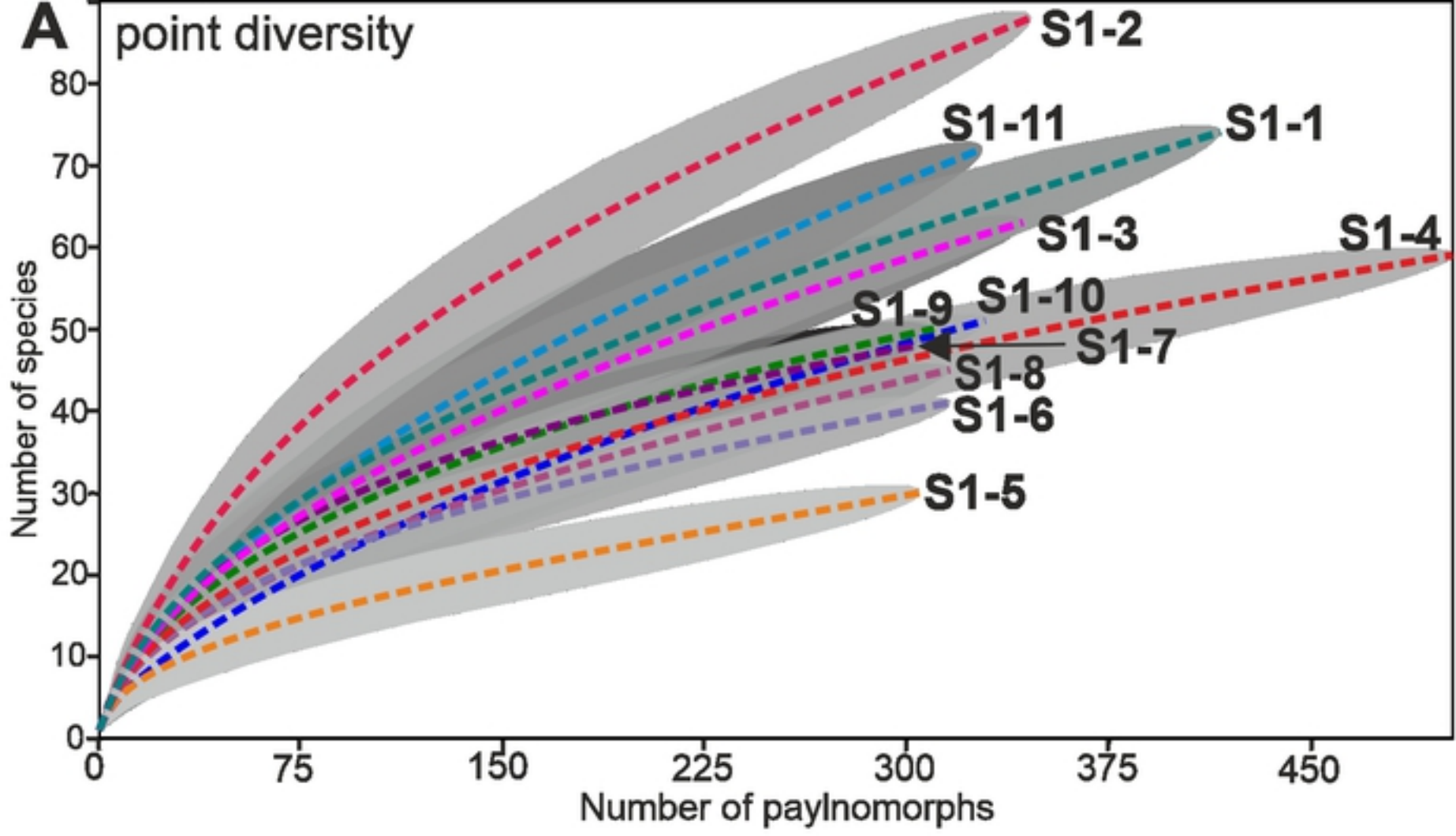

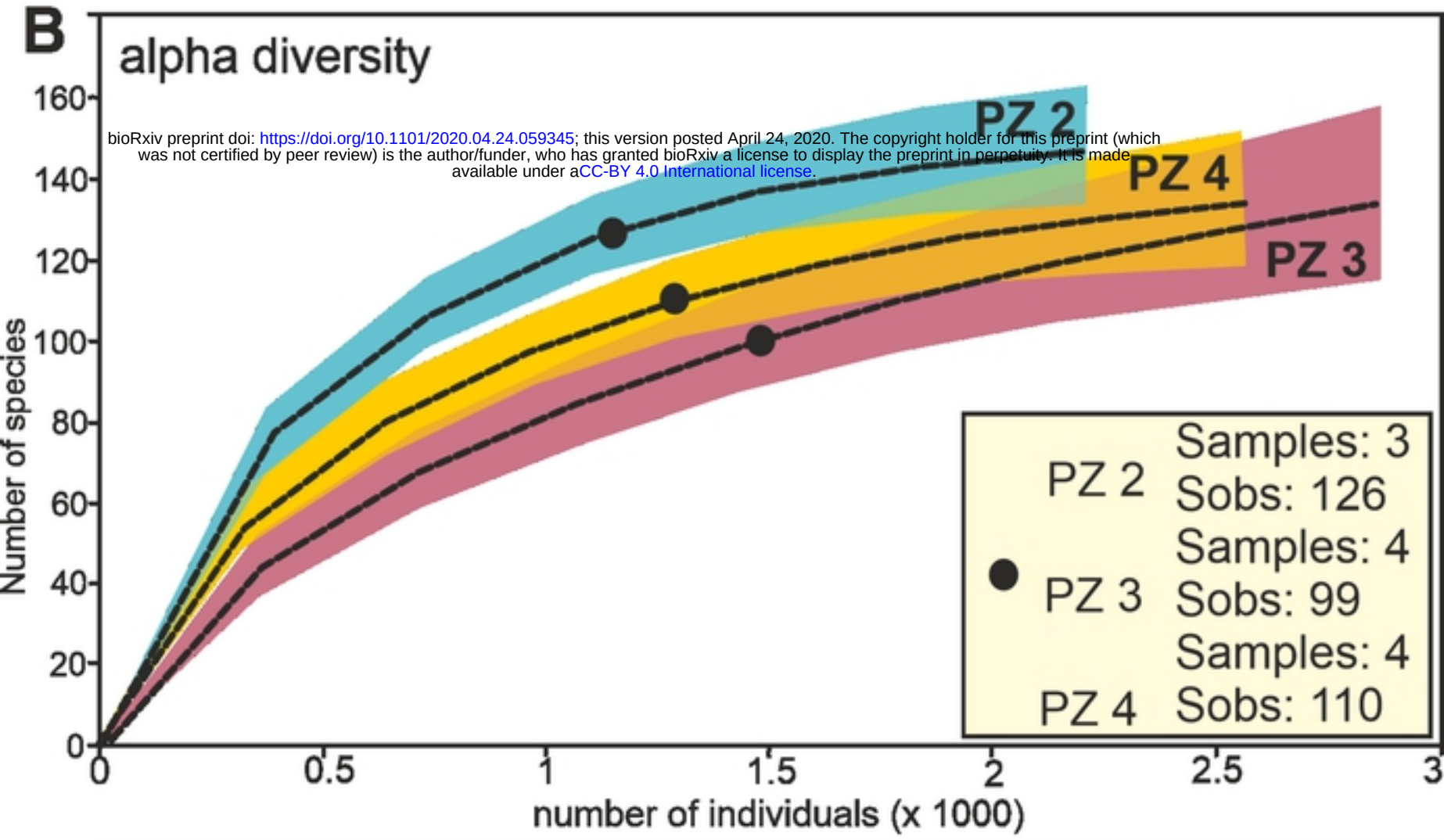

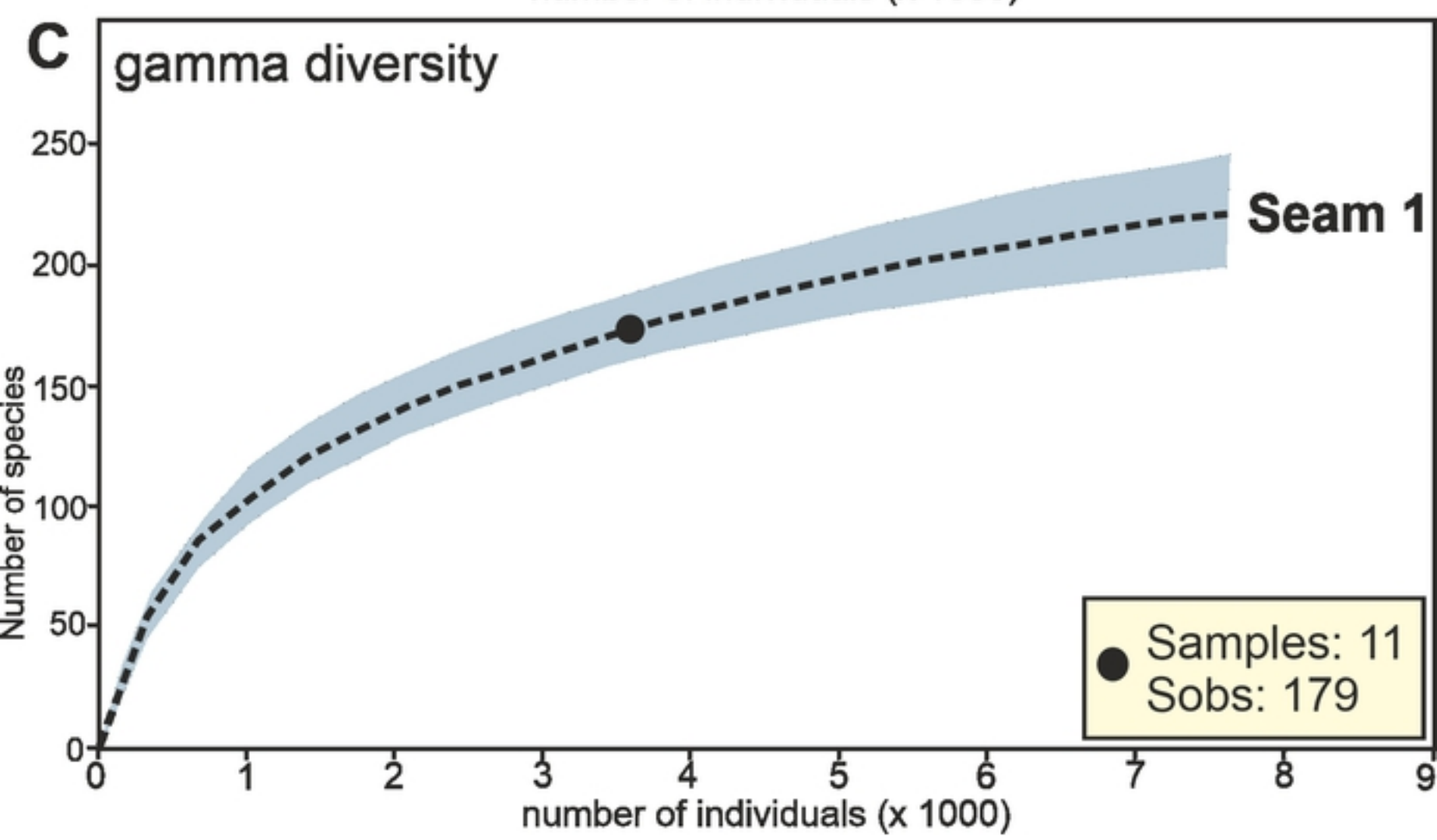

Figure 12

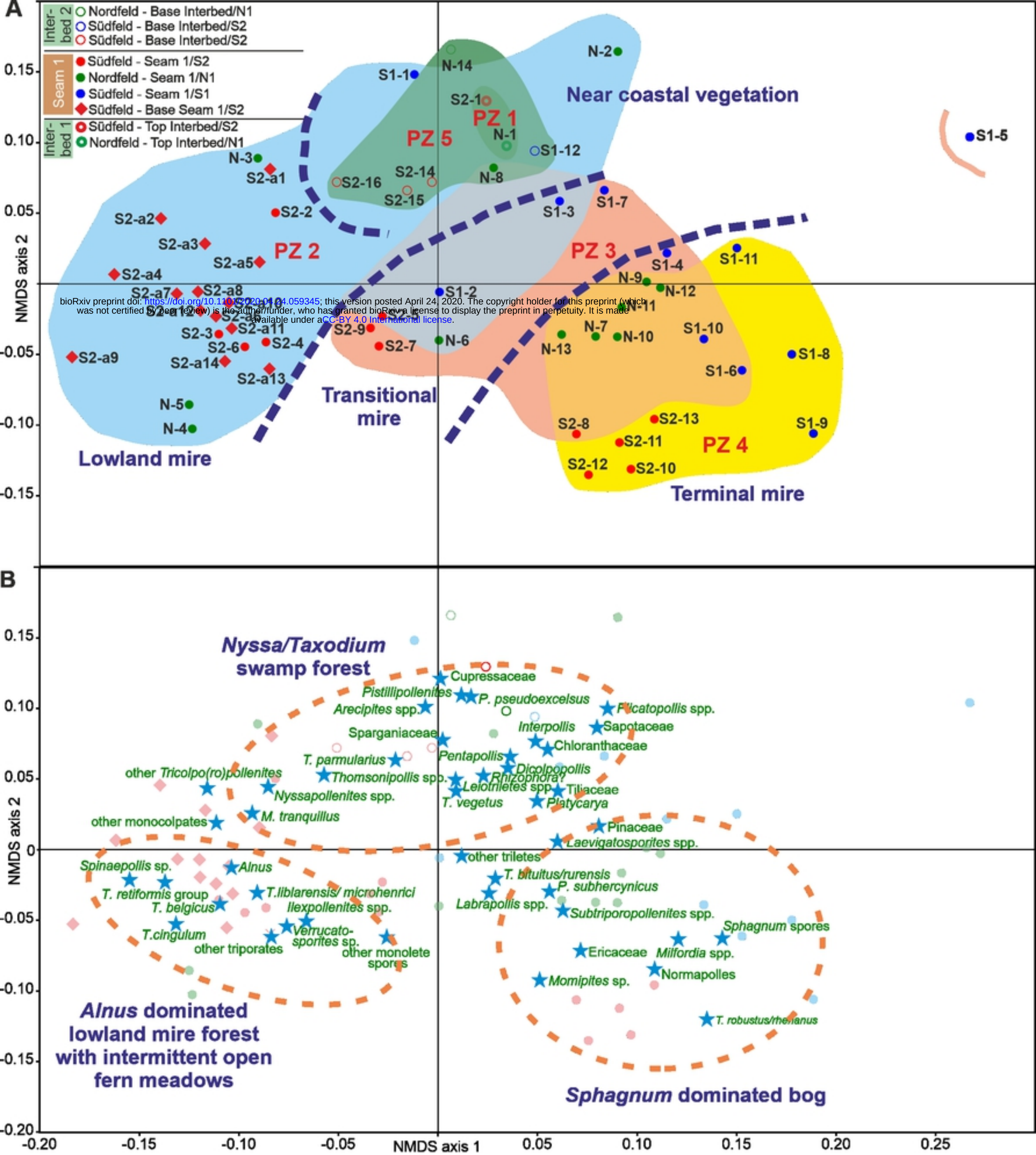

Figure 13

Figure 14